BMC Genomics

RESEARCH

Open Access

Sequence comparison of the mitochondrial genomes of five caridean shrimps of the infraorder Caridea: phylogenetic implications and divergence time estimation

Yuman Sun[1,2†], Wanting Liu[1†], Jian Chen[1], Jiji Li[1], Yingying Ye[1*] and Kaida Xu[3*]

Abstract

Background The Caridea, affiliated with Malacostraca, Decapoda, and Pleocyemata, constitute one of the most significant shrimp groups. They are widely distributed across diverse aquatic habitats worldwide, enriching their evolutionary history. In recent years, considerable attention has been focused on the classification and systematic evolution of Caridea, yet controversies still exist regarding the phylogenetic relationships among families.

Methods Here, the complete mitochondrial genome (mitogenome) sequences of five caridean species, namely *Heterocarpus sibogae*, *Procletes levicarina*, *Macrobrachium sp.*, *Latreutes anoplonyx*, and *Atya gabonensis*, were determined using second-generation high-throughput sequencing technology. The basic structural characteristics, nucleotide composition, amino acid content, and codon usage bias of their mitogenomes were analyzed. Selection pressure values of protein-coding genes (PCGs) in species within the families Pandalidae, Palaemonidae, and Atyidae were also computed. Phylogenetic trees based on the nucleotide and amino acid sequences of 13 PCGs from 103 caridean species were constructed, and divergence times for various families within Caridea were estimated.

Results The mitogenome of these five caridean species vary in length from 15,782 to 16,420 base pairs, encoding a total of 37 or 38 genes, including 13 PCGs, 2 rRNA genes, and 22 or 23 tRNA genes. Specifically, *L. anoplonyx* encodes an additional tRNA gene, bringing its total gene count to 38. The base composition of the mitogenomes of these five species exhibited a higher proportion of adenine-thymine (AT) bases. Six start codons and four stop codons were identified across the five species. Analysis of amino acid content and codon usage revealed variations among the five species. Analysis of selective pressure in Pandalidae, Palaemonidae, and Atyidae showed that the Ka/Ks values of PCGs in all three families were less than 1, indicating that purifying selection is influencing on their evolution. Phylogenetic analysis revealed that each family within Caridea is monophyletic. The results of gene rearrangement and phylogenetic analysis demonstrated correlations between these two aspects. Divergence time estimation, supported by fossil records, indicated that the divergence of Caridea species occurred in the Triassic period of the Mesozoic era, with subsequent differentiation into two major lineages during the Jurassic period.

†Yuman Sun and Wanting Liu contributed equally to this work.

*Correspondence:
Yingying Ye
yeyy@zjou.edu.cn
Kaida Xu
xkd1981@163.com
Full list of author information is available at the end of the article

Conclusions This study explored the fundamental characteristics and phylogenetic relationships of mitogenomes within the infraorder Caridea, providing valuable insights into their classification, interspecific evolutionary patterns, and the evolutionary status of various Caridea families. The findings provide essential references for identifying shrimp species and detecting significant gene rearrangements within the Caridea infraorder.

Keywords Mitochondrial genome, Caridea, Structural features, Gene rearrangement, Phylogenetic analysis, Divergence time

Background

The infraorder Caridea (Dana, 1852), belonging to the order Decapoda and the suborder Pleocyemata, is one of the largest infraorders within the Decapoda, comprising approximately 4,000 extant species [1]. Caridean species are found in all aquatic habitats worldwide, constituting one of the most significant global shrimp groups [2]. Caridean shrimps display a wide range of diverse morphological and physiological-biochemical characteristics across various aquatic habitats. For example, in tropical marine environments, many small caridean species have evolved unique lifestyles and form either temporary or long-term symbiotic relationships with various marine organisms [3], including cnidarians, sponges, mollusks, echinoderms, isopods, copepods, fish, and other crustaceans [4–9]. The diverse habitats and unique lifestyles of caridean species have led to a remarkable diversity in their appearances. Some caridean species possess completely transparent exoskeletons, while others boast vibrant colors that enhance their visual appeal. Additionally, certain caridean species can alter their body coloration, using pigment cells to mimic the substrate colors of their environment, thereby camouflaging themselves with the surrounding hues for adaptive advantages [10]. Unlike other shrimp taxa, Caridean shrimps have become a primary component in marine ornamental shrimp keeping, valued not only for their culinary qualities but also for their diverse lifestyles and striking appearances. Some species hold significant ornamental value, thus garnering high economic importance within the fisheries and aquaculture sectors [11].

In taxonomy, morphological characteristics such as the rostrum, pereopods, mouthparts, and the length-to-width ratio of abdominal segments are commonly used to delineate superfamilies and families within shrimp species [12, 13]. However, the correspondence between morphological classifications and natural monophyletic groups, i.e., whether they accurately reflect the systematic evolutionary relationships among populations, remains uncertain. The rapid advancement of modern molecular biology has significantly propelled research in molecular systematics. By investigating molecular sequences, this approach addresses the limitations of traditional taxonomy and resolves many contentious issues in classification and systematic evolution [14, 15]. For instance, multiple independent molecular studies have confirmed that the families Gnathophyllidae, Hymenoceridae, and Kakaducarididae are nested within Palaemonidae. These findings have prompted researchers to reevaluate the morphological characteristics of these families. Studies by Short et al. [16] and De Grave et al. [17] have further revealed shared morphological features between these three families and Palaemonidae. Consequently, they proposed that these families are effectively synonymous.

Current analysis of Caridea phylogenetics are marked by ongoing disputes regarding the classification of certain species, with researchers obtaining varied phylogenetic results from different molecular sequences and tree construction methods. Bracken et al. [18] conducted a phylogenetic analysis using mitochondrial and nuclear gene sequences (*16S rRNA* + *18S rRNA*), which supported the monophyly of Alvinocarididae, Pandalidae, and Atyidae representing the basal lineage of Caridea, while Oplophoridae appeared to be paraphyletic. Li et al. [19], using five nuclear gene sequences (*enolase*, *H3, NaK*, *PEPCK*, and *I8S rRNA*), also supported the notion that Atyidae represents the basal lineage of Caridea. Additionally, they suggested that Hippolytidae and Palaemonidae are paraphyletic. However, Ye et al. [20], utilizing 13 mitochondrial protein-coding genes (PCGs), supported the monophyly of Hippolytidae and Palaemonidae, but did not support Atyidae as the basal lineage of Caridea. Additionally, Sun et al. [21], using 13 mitochondrial PCGs, confirmed the monophyly of Palaemonidae. At the genus level, the polyphyly of *Plesionika* and *Heterocarpus* within the family Pandalidae has been a research focus. Kong et al. [1], conducting phylogenetic analyses based on 13 PCGs, concluded that *Plesionika* was polyphyletic while *Heterocarpus* was monophyletic. However, Wang et al. [14], using 13 PCGs from mitogenomes, concluded that both Plesionika and Heterocarpus were polyphyletic. Similarly, Liao et al. [22], utilizing sequences from two mitochondrial genes (*12S* and *16S rRNA*) and six nuclear genes (*H3*, *NaK*, *enolase*, *PEPCK*, *atpβ*, and *GAPDH*), also found support for the polyphyly of *Plesionika* and *Heterocarpus* in their phylogenetic analyses. Furthermore, controversies continue regarding the intra-familial and intra-specific phylogenetic relationships

within Caridea. Most studies based on mitochondrial sequences support the sister relationship between Pandalidae and Palaemonidae. However, in the study by Li et al. [19], Pandalidae and Palaemonidae appeared in two separate clades, indicating a distant relationship. Tan et al. [23] and Wang et al. [24], using 13 PCGs and a combination of 13 PCGs with *16S rRNA* and *12S rRNA* respectively, supported Atyidae and Alvinocarididae as sister groups. In contrast, Liu et al. [25], using 13 PCGs and Maximum Likelihood (ML) analysis, concluded that Pandalidae and Alvinocarididae are sister groups to each other. Cronin et al. [26] and Kong et al. [1], using Bayesian inference (BI) based on 13 PCGs, revealed that Alvinocarididae, Acanthephyridae, Oplophoridae, Nematocarcinidae, and Atyidae form a close-knit clade. Chak et al. [27], using the same gene sequences and tree construction methods, supported the findings of Cronin et al. [26] and Kong et al. [1]; however, they noted that Atyidae did not cluster with these four families in the ML phylogenetic tree. Additionally, the results from Wang et al., based on 13 PCGs and using both BI and ML methods, further supported the close relationship among Alvinocarididae, Acanthephyridae, Oplophoridae, and Nematocarcinidae [14].

The mitochondrial genome (mitogenome), characterized by maternal inheritance, high mutation rate, and rapid gene evolution, is an ideal molecular marker for studies on population genetic structure, genome evolution, species identification, and phylogenetics [28, 29]. Compared to short sequences of single genes, the complete mitogenome provides a richer repository of biological information for deciphering evolutionary relationships, including patterns controlling replication and transcription, gene arrangement, positional information, and RNA secondary structure. With the assistance of this biological information, reconstructed phylogenetic trees became more reliable [30–32]. However, the current availability of complete mitogenome for Caridea is limited. As of February 19, 2024, the GenBank database contained only 98 complete mitogenome sequences of caridean species, excluding unverified sequences. Moreover, data collection has been unevenly distributed. Pandalidae and Palaemonidae have fewer available sequences compared to Atyidae, and Hippolytidae has data for only one species.

This study aimed to sequence the complete mitogenomes of five caridean species, thereby enriching the Caridea database. These species include *Heterocarpus sibogae* and *Procletes levicarina* from the family Pandalidae, *Macrobrachium sp.* from the family Palaemonidae, *Latreutes anoplonyx* from the family Hippolytidae, and *Atya gabonensis* from the family Atyidae. The basic characteristics of the mitogenomes of these caridean species were analyzed. Additionally, genetic rearrangement patterns among different species within each family were explored through mitogenome alignment. This analysis aimed to understand their genetic traits and the evolutionary patterns among families. The reconstruction of the Caridea phylogenetic tree was conducted using sequences of the 13 mitochondrial PCGs, enabling a systematic analysis to infer or evaluate the evolutionary relationships among Caridea families and genera. Additionally, the taxonomic attribution of these species was investigated to elucidate their origins and phylogenetic patterns, providing valuable insights for the identification of caridean species and the breeding of economically important shrimp species in the aquaculture industry.

Materials and methods

Sampling, identification and DNA extraction

This study collected samples from five caridean species, as detailed in Table 1. Four species were collected from southeastern China's coastal waters: *P. levicarina*, *L. anoplonyx*, and *Macrobrachium sp*. from Zhoushan, Zhejiang, and *H. sibogae* from Taizhou, Zhejiang. *A. gabonensis* was acquired from the Tianjin Aquarium Market. Preliminary morphological identifications were conducted by consulting taxonomic experts at the Zhejiang Ocean University Biological Museum and by referring to Volume 36 and Volume 44 of the "Fauna Sinica" [12, 13], and "Zhejiang Fauna: Crustacea" [33]. Muscle tissue from the abdominal segments of the five caridean species was dissected for DNA extraction and stored in anhydrous ethanol prior to extraction. Total genomic DNA of the five caridean species was extracted using the salting-out method [34]. Its quality was assessed by 1% agarose gel electrophoresis, and the extracted DNA was stored at − 20 °C. Subsequently, the *cox1* and *16S rRNA*

Table 1 Annotation of five caridean complete mitochondrial genomes

Family	Species	Sampling date	Species location
Pandalidae	*Heterocarpus sibogae*	April 2021	Zhoushan, Zhejiang Province
	Procletes levicarina	April 2022	Zhoushan, Zhejiang Province
Palaemonidae	*Macrobrachium sp.*	September 2021	Zhoushan, Zhejiang Province
Hippolytidae	*Latreutes anoplonyx*	April 2022	Zhoushan, Zhejiang Province
Atyidae	*Atya gabonensis*	July 2022	Tianjin

gene sequences of each sample were amplified. Sequence alignments were performed using the NCBI database's Blast function [35] to confirm the species identity.

Mitogenomes sequencing, assembly, and annotation

The mitogenomes of these samples were sequenced using second-generation high-throughput technology on the Illumina HiSeqTM platform at Shanghai Yuanshen Biomedical Technology Co., Ltd. Before sequencing, the genomic DNA samples were subjected to electrophoresis in a 1% agarose gel to assess quality. DNA concentration and purity were then quantified using a NanoDrop 2000 spectrophotometer. After the DNA passed the quality check, 1 μg was used to construct the library. For library preparation, the DNA was fragmented into 300–500 bp pieces using the Covaris M220 instrument through ultrasonication. After the DNA fragments were purified, sequencing libraries were assembled. Following sequencing, which generated 10G of data, the raw data underwent filtration to remove adapters, low-quality and duplicate reads, sequences with high N rates, and any sequences shorter than 50 bp, yielding high-quality (clean) sequencing data. The sequencing reads were iteratively assembled multiple times using GetOrganelle (https://github.com/Kinggerm/GetOrganelle) [36], producing preliminary assembly results. High-quality sequencing reads were then aligned to the mitochondrial genome sequences for base correction using Pilon v1.23 [37]. Subsequently, the assembled mitochondrial genomes were annotated using MITOS2 (http://mitos2.bioinf.uni-leipzig.de/index.py) [38], utilizing the invertebrate codon table for accurate annotation.

Sequence analysis

The complete mitogenome data of five caridean species were uploaded to the GenBank database with the following accession numbers: *H. sibogae* OP380621, *P. levicarina* OR120370, *Macrobrachium sp*. OQ512153, *A. gabonensis* OP650929, and *L. anoplonyx* OR120369. Additionally, the raw genome sequencing datasets for these species were submitted to the NCBI Sequence Read Archive (SRA) under accession number PRJNA1123500. The complete genome sequences of the five caridean species were annotated using Sequin software (http://www.ncbi.nlm.nih.gov/Sequin/) [39]. Circular maps of their mitogenomes were generated using the Proksee server (https://proksee.ca/). MEGA-X [40] was employed to determine the nucleotide composition, amino acid content, and relative synonymous codon usage (RSCU) of the 13 PCGs in the mitochondrial genomes of the caridean species. The AT-skew and GC-skew were calculated using the formulas AT-skew = (A − T)/(A + T) and GC-skew = (G − C)/(G + C) [41]. Tandem repeat sequences in the control region were identified using Tandem Repeat Finder v4.09 [42]. All tRNA genes were identified and their secondary structures were predicted using the online software MITOS2 [38]. Complete mitogenome sequences of 11 Pandalidae species, 20 Palaemonidae species, and 27 Atyidae species were downloaded from the GenBank database for selective pressure analysis (Table S1). DAMBE 7 [43] was utilized to identify the sequences of the 13 PCGs for each species. MEGA-X conducted single-gene alignments for species within the three families [40]. The ratio of nonsynonymous to synonymous substitutions (Ka/Ks) was calculated using DnaSP v6.12.01 [44].

Gene order analysis

In addition to the five species sequenced in this study, 98 caridean mitogenomes were downloaded from the GenBank database (Table S1) for comparative analysis. To identify gene arrangement patterns not previously detected in caridean species, the gene arrangement sequences of all 103 mitogenomes were compared with those of ancestral Decapoda. To verify that differences in gene arrangement were not due to annotation errors, all mitogenomes exhibiting gene rearrangement were re-annotated using MITOS2 [38]. The correctly annotated mitogenomes can be accessed as linear mitochondrial gene maps from the MPI-MP website CHLOROBOX-OGDRAW (https://chlorobox.mpimp-golm.mpg.de/OGDraw.html#).

Phylogenetic analysis

To investigate the phylogenetic relationships within the infraorder Caridea, a phylogenetic tree was constructed using mitogenome sequences of 103 caridean species, including five newly sequenced species and an additional 98 caridean species obtained from the GenBank database (Table S1). *Litopenaeus stylirostris* (EU517503) and *Marsupenaeus japonicus* (MG772559) from Penaeidae were selected as outgroups. Phylogenetic analysis of 105 species was conducted using the 13 PCGs. DAMBE 7 [43] was used to identify the 13 PCGs sequences for each species. The nucleotide and amino acid sequences of all 13 PCGs were individually aligned using the default settings of ClustalW in MEGA X [40], and then concatenated using PhyloSuite [45]. Gblocks v.0.91b [46] was employed to eliminate divergent and ambiguous regions, selecting conserved regions with default parameters. Subsequently, DAMBE 7 [43] was used to compute substitution saturation under the GTR substitution model to assess the suitability of these sequences for phylogenetic tree construction. Two data matrices, the nucleotide sequence matrix (PCGnt) and the amino acid sequence matrix (PCGaa), were obtained for phylogenetic analysis.

Two methods were employed to analyze phylogenetic relationships within the infraorder Caridea: the Maximum Likelihood (ML) method using IQ tree 2.1.3 [47] and the Bayesian inference (BI) method using MrBayes 3.2.7a [48]. For the BI analysis, sequence files were converted using PAUP 4 [49], followed by model selection based on the Akaike Information Criterion (AIC) using MrMTgui in combination with PAUP 4, ModelTest 3.7 [50], and MRModelTest 2.3 [51] programs (GTR + I + G). BI tree analysis was conducted using four simultaneous Markov chains (MCMC), including one cold chain and three hot chains. The analysis ran for 2 million generations, sampling every 1000 generations. The first 25% of the data was discarded as burn-in, and convergence was assessed by the mean standard deviation of split frequencies (< 0.01). ML tree reconstruction was performed using the same dataset. ModelFinder [52] was used to select the optimal nucleotide substitution model (TIM2 + F + R8) and the best amino acid substitution model (Q.bird + F + R9). Bootstrap values were set to 1000 to reconstruct the consensus tree. FigTree v1.4.3 [53] was used for visualizing and editing the phylogenetic trees, with additional refinements made in Photoshop.

Estimation of divergence times analysis

Divergence times within Caridea were estimated using BEAST v1.10.4 software [54], based on 13 PCGs from 103 caridean species (Table S1). The time tree's branch evolution rate was modeled using the Yule process, with an uncorrelated relaxed clock applied to the molecular clock model. Fossil calibration points were assigned using a normal distribution as the prior. Two fossil calibration points from the TimeTree knowledge base (http://www.timetree.org/) were used: the divergence between *Palaemon* and *Macrobrachium* at 141 Mya, and between Alpheidae and Palaemonidae at 185 Mya, each with a standard deviation of 2.0. The MCMC was run for 200 million generations, sampling every 1000 generations, across three independent runs, with results combined using Logcombiner. Twenty-five percent of the burn-in was removed using TreeAnnotator v1.10.4.Chain convergence was confirmed with Tracer v.1.7.2 [55], with all parameter ESSs exceeding 200. Fossil records from Timetree and previous studies [11, 21] validated the divergence time estimates. Finally, the estimated time tree was edited and annotated using FigTree v1.4.3 [53].

Results

Genome structure, composition, and skewness

The lengths of complete mitogenome sequences of five caridean species are: 16,036 bp for *H. sibogae*, 15,889 bp for *P. levicarina*, 15,782 bp for *Macrobrachium sp.*, 16,420 bp for *L. anoplonyx*, and 15,978 bp for *A. gabonensis* (Fig. 1). Except for *L. anoplonyx*, the mitogenomes of the other four species encoded 37 genes, including 13 PCGs, 22 tRNAs, 2 rRNAs, and a CR. A duplication was observed in *trnD* of *L. anoplonyx*, resulting in a total of 38 genes. All five species had 14 genes encoded on the L strand, including 4 PCGs (*nad5*, *nad4*, *nad4l*, and *nad1*), 8 tRNAs (*trnF*, *trnH*, *trnP*, *trnL1*, *trnV*, *trnQ*, *trnC*, and *trnY*), and 2 rRNAs (*16S rRNA* and *12S rRNA*). On the H strand, *H. sibogae*, *P. levicarina*, *Macrobrachium sp.*, and *A. gabonensis* each encode 23 genes: 9 PCGs (*cox1*, *cox2*, *atp8*, *atp6*, *cox3*, *nad3*, *nad6*, *cob*, *nad2*) and 14 tRNAs (*trnL2*, *trnK*, *trnD*, *trnG*, *trnA*, *trnR*, *trnN*, *trnS1*, *trnE*, *trnT*, *trnS2*, *trnI*, *trnM*, *trnW*). *L. anoplonyx* encodes an additional *trnD* gene, bringing the total to 24 on the H strand (Table 2).

The base composition of the mitogenomes of five caridean species varied, with A ranging from 33.18% to 36.75%, T from 27.04% to 35.78%, G from 11.94% to 13.36%, and C from 19.10% to 24.98%. The AT content ranged from 61.66% to 68.96%,, indicating a bias towards codons containing A and T. Base skewness calculations showed positive AT-skew for all species except. The AT skew values for all five species ranged from − 0.038 to 0.147, and GC skew values from − 0.303 to − 0.225 (Fig. 2).

Codon usage and amino acid composition

The total lengths of PCGs in the mitogenomes of the five caridean species were as follows: 11,143 bp for *H. sibogae*, 11,121 bp for *P. levicarina*, 11,071 bp for *Macrobrachium sp.*, 11,113 bp for *L. anoplonyx*, and 11,093 bp for *A. gabonensis*. The longest PCG among these species was *nad5*, ranging from 1692 to 1718 bp, while the shortest was the *atp8* gene, ranging from 159 to 165 bp. These species' PCGs showed a relatively high AT content, with *L. anoplonyx* having the highest at 66.17%. The AT-skew of PCGs was negative in all five species, ranging from − 0.169 to − 0.149. Comparison of start and stop codons across all PCGs revealed six start and four stop codons in these species (Table 3). Most PCGs began with ATG, ATT, ATA, ATC, or ACG, except *cox1* in *A. gabonensis*, which started with CCG. Most PCGs ended with TAA or TAG, with two showing incomplete stop codons: TA(A) and T(AA).

Amino acid content and codon usage were analyzed and compared across five caridean species (Fig. 3). In *H. sibogae*, the amino acid with the highest content was Leu1, at 8.18%; while the lowest was Cys, at 1.39%. For *P. levicarina*, the highest content was also Leu1, at 7.88%; and the lowest was Arg, at 1.43%. In *Macrobrachium sp.*, the highest content was Thr, at 8.01%; and the lowest was Cys, at 1.35%. *L. anoplonyx* exhibited the highest content of Phe, at 8.63%; while the lowest was Glu, at 1.09%. In

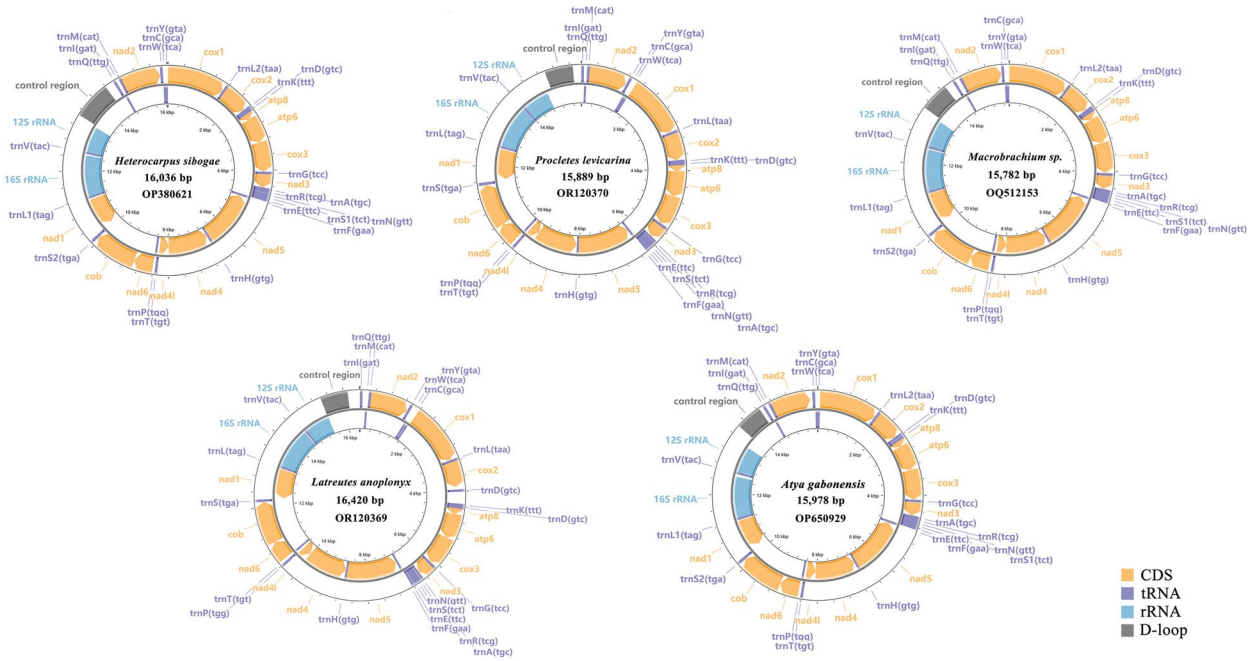

Fig. 1 Circle map of mitogenome composition of five caridean species

A. gabonensis, the highest content was Leu1, at 9.08%; and the lowest was Cys, at 1.10%. RSCU represents the relative frequency of a specific codon encoding an amino acid, excluding the influence of amino acid composition. When RSCU = 1, it indicates no codon preference; RSCU > 1 indicates higher frequency, while RSCU < 1 indicates lower frequency. Most used codons across the five species varied, with TTA (Leu) and GGA (Gly) being notably frequent. Specific patterns include *H. sibogae* favoring TTA, GTA (Val), TCT (Ser); *P. levicarina* and *L. anoplonyx* also starting with TTA; *Macrobrachium sp.* leading with GGA; and *A. gabonensis* with GGA, TCA (Ser), CTA (Leu). The least frequently used codons across all five species were GCG (Ala), ACG (Thr), TCG (Ser), and CCG (Pro).

Transfer and ribosomal RNAs

The total lengths of tRNA genes in the mitogenomes of five caridean species were 1,461 bp (*H. sibogae*), 1,462 bp (*P. levicarina*), 1,453 bp (*Macrobrachium sp.*), 1,580 bp (*L. anoplonyx*), and 1,464 bp (*A. gabonensis*). The lengths of all tRNA genes in these species ranged from 62 to 72 bp (Table 2). All tRNA genes in these species showed high AT content: 65.16% in *H. sibogae*, 67.38% in *P. levicarina*, 64.49% in *Macrobrachium sp.*, 71.52% in *L. anoplonyx*, and 64.82% in *A. gabonensis*. Comparative analysis revealed that in all species except *L. anoplonyx*, the *trnS1* gene lacked the DHU arm. In *L. anoplonyx*, the *trnS2* gene was the one missing the DHU arm (Fig. 4). Additionally, specific genes lacked the TψC loop: *trnF*, *trnM*, and *trnP* in *H. sibogae*; *trnA*, *trnF*, *trnH*, and *trnR* in *P. levicarina* and *Macrobrachium sp.*; *trnF* in *L. anoplonyx*; and *trnY* in *A. gabonensis*. Furthermore, the other tRNA genes in all five species formed typical cloverleaf structures.

The total lengths of the *16S rRNA* and *12S rRNA* genes were similar among the five species, with the length of *16S rRNA* ranging from 1,284 to 1,336 bp and the length of *12S rRNA* ranging from 793 to 803 bp (Table 2). The *16S rRNA* and *12S rRNA* genes in all five species were located between *trnL1* and *trnI*, separated by *trnV*. The rRNA genes in all five species exhibited high AT content, ranging from 65.25% to 71.52% (Fig. 2).

Control region

In the mitogenomes of five caridean species, the length of the CR ranged from 649 to 942 bp, all located between the *12S rRNA* and *trnI* (Table 2). The CR in these five species exhibited pronounced biases in nucleotide composition, with a high prevalence of AT bases (Fig. 2). The AT content was notably high, with *H. sibogae* at 80.79%, *P. levicarina* at 78.48%, *Macrobrachium sp.* at 81.98%, *L. anoplonyx* at 81.60%, and *A. gabonensis* at 80.28%, all significantly exceeding their respective GC contents.

Additionally, tandem repeat sequences were identified in the CR of *H. sibogae*, *Macrobrachium sp.*, and *L. anoplonyx* (Table S2). The CR of *H. sibogae* contained a tandem repeat unit size of 155 bp, repeated twice. The CR

Table 2 Annotation of five caridean complete mitochondrial genomes

Feature	Strand	Location										Size (bp)				
		H. sibogae		*P. levicarina*		*Macrobrachium sp.*		*L. anoplonyx*		*A. gabonensis*		*H. sibogae*	*P. levicarina*	*Macrobrachium sp.*	*L. anoplonyx*	*A. gabonensis*
		from	to	from	to	from	to	from	to	from	to					
cox1	+	1	1,539	1,437	2,972	1	1,535	1,592	3,130	67	1,599	1,539	1,536	1,535	1,539	1,533
trnL2(taa)	+	1,535	1,600	2,975	3,040	1,536	1,599	3,134	3,198	1,602	1,665	66	66	64	65	64
cox2	+	1,604	2,291	3,045	3,729	1,603	2,287	3,200	3,880	1,669	2,356	688	685	685	681	688
trnD(gtc)	+	/	/	/	/	/	/	3,950	4,011	/	/	/	/	/	62	/
trnK(ttt)	+	2,292	2,359	3,733	3,799	2,288	2,355	4,324	4,392	2,357	2,424	68	67	68	69	68
trnD(gtc)	+	2,361	2,425	3,800	3,865	2,357	2,421	4,392	4,455	2,431	2,496	65	66	65	64	66
atp8	+	2,426	2,584	3,866	4,024	2,422	2,580	4,456	4,620	2,497	2,655	159	159	159	165	159
atp6	+	2,578	3,252	4,018	4,692	2,574	3,248	4,614	5,291	2,649	3,323	675	675	675	678	675
cox3	+	3,252	4,040	4,692	5,480	3,248	4,036	5,291	6,079	3,323	4,111	789	789	789	789	789
trnG(tcc)	+	4,044	4,108	5,484	5,548	4,043	4,107	6,086	6,148	4,115	4,179	65	65	65	63	65
nad3	+	4,109	4,462	5,549	5,902	4,114	4,461	6,149	6,502	4,189	4,533	354	354	348	354	345
trnA(tgc)	+	4,462	4,525	5,904	5,967	4,462	4,524	6,502	6,564	4,532	4,595	64	64	63	63	64
trnR(tcg)	+	4,525	4,590	5972	6,037	4,524	4,585	6,574	6,638	4,595	4,658	66	66	62	65	64
trnN(gtt)	+	4,595	4,659	6,038	6,102	4,588	4,653	6,639	6,706	4,659	4,725	65	65	66	68	67
trnS1(tct)	+	4,660	4,727	6,102	6,168	4,654	4,720	6,707	6,774	4,726	4,792	68	67	67	68	67
trnE(ttc)	+	4,728	4,796	6,169	6,238	4,721	4,789	6,783	6,849	4,793	4,860	69	70	69	67	68
trnF(gaa)	−	4,795	4,860	6,237	6,302	4,793	4,858	6,848	6,913	4,859	4,926	66	66	66	66	68
nad5	−	4,858	6,574	6,283	7,980	4,861	6,552	6,917	8,611	4,928	6,619	1,717	1,698	1,692	1,695	1,692
trnH(gtg)	−	6,587	6,652	8,029	8,094	6,586	6,649	8,633	8,696	6,656	6,720	66	66	64	64	65
nad4	−	6,659	7,991	8,095	9,433	6,652	7,986	8,703	10,038	6,724	8,059	1,333	1,339	1,335	1,336	1,336
nad4l	−	7,985	8,284	9,427	9,726	7,980	8,279	10,053	10,349	8053	8,355	300	300	300	297	303
trnT(tgt)	+	8,286	8,350	9,728	9,790	8,282	8,347	10,351	10,416	8,358	8,422	65	63	66	66	65
trnP(tgg)	−	8,351	8,416	9,791	9,855	8,347	8,413	10,418	10,482	8,423	8,488	66	65	67	65	66
nad6	+	8,419	8,934	9,858	10,373	8,448	8,930	10,511	11,005	8,518	9,006	516	516	483	495	489
cob	+	8,934	10,068	10,373	11,507	8,930	10,064	11,005	12,141	9,011	10,147	1,135	1,135	1,135	1,137	1,137
trnS2(tga)	+	10,069	10,140	11,508	11,579	10,065	10,133	12,141	12,206	10,146	10,215	72	72	69	66	70
nad1	−	10,162	11,100	11,602	12,540	10,154	11,092	12,208	13,131	10,236	11,177	939	939	939	924	942
trnL1(tag)	−	11,148	11,213	12,576	12,641	11,112	11,177	13,185	13,249	11,212	11,278	66	66	66	65	67
16S	−	11,208	12,491	12,623	13,958	11,137	12,444	13,231	14,537	11,236	12,557	1,284	1,336	1,308	1,307	1,322
trnV(tac)	−	12,537	12,600	13,964	14,028	12,479	12,546	14,560	14,626	12,635	12,702	64	65	68	67	68
12S	−	12,601	13,394	14,032	14,832	12,546	13,348	14,625	15,417	12,706	13,504	794	801	803	793	799
CR	+	13,459	14,400	14,984	15,680	13,425	14,123	15,411	16,111	13,820	14,468	942	697	699	701	649
trnI(gat)	+	14,625	14,691	1	67	14,339	14,405	1	67	14,563	14,629	67	67	67	67	67
trnQ(ttg)	−	14,705	14,772	83	150	14,440	14,507	157	222	14,639	14,706	68	68	68	66	68
trnM(cat)	+	14,772	14,836	150	216	14,519	14,585	232	298	14,714	14,779	65	67	67	67	66

Table 2 (continued)

Feature	Strand	Location										Size (bp)				
		H. sibogae		*P. levicarina*		*Macrobrachium sp.*		*L. anoplonyx*		*A. gabonensis*		*H. sibogae*	*P. levicarina*	*Macrobrachium sp.*	*L. anoplonyx*	*A. gabonensis*
		from	to	from	to	from	to	from	to	from	to					
nad2	+	14,837	15,838	217	1,212	14,586	15,581	299	1,321	14,780	15,784	1,002	996	996	1,023	1,005
trnW(tca)	+	15,837	15,905	1,226	1,294	15,585	15,653	1,330	1,396	15,843	15,912	69	69	69	67	70
trnC(gca)	−	15,906	15,972	1,305	1,372	15,656	15,718	1,430	1,502	15,912	15,977	67	68	63	73	66
trnY(gta)	−	15,973	16,036	1,373	1,436	15,719	15,782	1,512	1,578	1	65	64	64	64	67	65

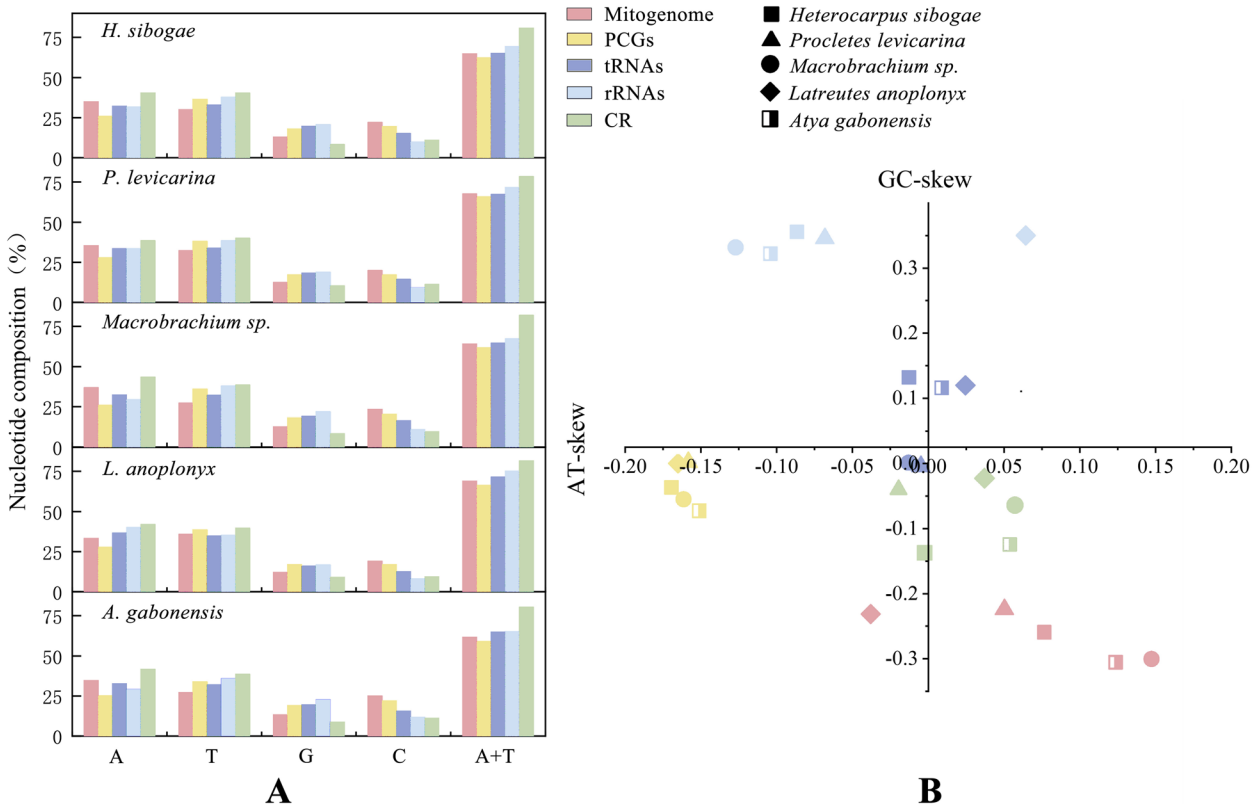

Fig. 2 Nucleotide composition (**A**) and nucleotide skews (**B**) of five newly sequenced caridean mitogenomes

of *Macrobrachium sp*. featured a tandem repeat sequence 'TCTTATAAAACTTATAG' of 17 bp, repeated nearly twice. The CR of *L. anoplonyx* harbored a tandem repeat sequence with a repeat unit size of 70 bp, repeated 2.5 times.

Selective pressure analysis

The Ka/Ks ratio, which measures the ratio of nonsynonymous to synonymous substitutions, is used in genetics to analyze gene variation and selection pressures during species evolution [31]. Generally, a Ka/Ks ratio greater than 1 indicates positive selection, a ratio of 1 suggests neutral selection, and a ratio less than 1 implies purifying selection [20]. This study involved sequencing four caridean families. Due to the limited availability of mitogenome data for Hippolytidae (only two sequences), selective pressure analysis was exclusively performed on the 13 PCGs of species from the three families: Pandalidae, Palaemonidae, and Atyidae. Differences in selective pressure on PCGs were observed among species, including newly sequenced ones *(H. sibogae*, *P. levicarina*, *Macrobrachium sp.*, and *A. gabonensis*) and others from GenBank, across Pandalidae, Palaemonidae, and Atyidae. Synonymous and nonsynonymous substitution rates and their ratios were calculated for each species, and bar and line graphs were constructed to explore the relationship between evolution and selection pressure (Fig. 5).

The result indicated that the Ka/Ks values of PCGs in 13 Pandalidae species ranged from 0.067 to 0.358 (Fig. 5A). In Pandalidae, the lowest Ka/Ks value was 0.067 for *cox1*, indicating high selection pressure, while *atp8* had the highest at 0.358, suggesting lower selection pressures on *atp8*, *nad6*, *nad2*, *nad4l*, and *nad5*. The result for Palaemonidae showed that the Ka/Ks values of the 13 PCGs from 21 species ranged between 0.118 and 0.456 (Fig. 5B). The *cox3* gene exhibited the lowest Ka/Ks value of 0.118, indicating the highest selection pressure on *cox3*, followed by *cox2*, *cox1*, *cob*, and *nad1* (with Ka/Ks values of 0.135, 0.146, 0.155, and 0.187, respectively). *Nad6* had the highest Ka/Ks value at 0.456 in Palaemonidae, indicating lower selection pressures, particularly on genes like *atp8*, *nad2*, and others. The result for Atyidae showed that the Ka/Ks values of the 13 PCGs from 28 species ranged between 0.072 and 0.421 (Fig. 5C). The *cox1* gene exhibited the lowest Ka/Ks value of 0.072, indicating the highest selection pressure on *cox1*, followed by *cox3*, *cob*, *cox2*, and *atp6* (with Ka/Ks values of 0.084, 0.124, 0.144, and 0.158, respectively). Atyidae's highest Ka/Ks value was 0.421 for *atp8*, suggesting lower selection pressures on *nad6*, *nad2*, and subsequent genes.

Table 3 The starting and ending codons of five caridean mitogenomes

Gene	Starting codons/Ending codons				
	H. sibogae	***P. levicarina***	***Macrobrachium sp.***	***L. anoplonyx***	***A. gabonensis***
cox1	ACG/TAA	ACG/TAA	ACG/TA(A)	ATT/TAA	CCG/TAA
cox2	ATG/TAA	ATG/T(AA)	ATG/T(AA)	ATG/TAA	ATG/T(AA)
atp8	ATC/TAA	ATT/TAA	ATC/TAA	ATT/TAG	ATT/TAA
atp6	ATG/TAA	ATG/TAA	ATG/TAA	ATG/TAA	ATG/TAA
cox3	ATG/TAA	ATG/TAA	ATG/TAA	ATG/TAA	ATG/TAA
nad3	ATT/TAG	ATT/TAA	ATT/TAA	ATT/TAA	ATA/TAA
nad5	ATT/TAA	ATT/TAG	ATG/TAA	ATT/TAA	ATT/TAA
nad4	ATG/TAA	ATG/T(AA)	ATG/TAA	ATG/T(AA)	ATG/T(AA)
nad4l	ATG/TAA	ATG/TAA	ATG/TAA	ATG/TAA	ATG/TAA
nad6	ATT/TAA	ATT/TAA	ATA/TAA	ATA/TAA	ATT/TAA
cob	ATG/TAA	ATG/T(AA)	ATG/T(AA)	ATG/TAA	ATG/TAG
nad1	ATA/TAG	ATA/TAA	ATG/TAG	ATT/TAA	ATT/TAA
nad2	ATT/TAA	ATT/TAA	ATT/TAG	ATT/TAA	ATT/TAG

Additionally, all Ka/Ks ratios for the 13 PCGs across the three families were below 1, indicating purifying selection throughout their evolutionary process.

Gene order

Alongside the five newly sequenced species, 98 caridean mitogenome sequences were downloaded from NCBI. Using *cox1* as the reference, gene arrangements in 103 caridean species across 13 families were compared to those of ancestral Decapoda. Mitochondrial gene arrangements in Atyidae, Glyphocrangonidae, Alvinocarididae, Acanthephyridae, Oplophoridae, and Nematocarcinidae matched those of ancestral Decapoda. However, 14 gene rearrangement patterns were identified in seven other Caridea families (Pandalidae, Palaemonidae, Hippolytidae, Thoridae, Alpheidae, Lysmatidae, Rhynchocinetidae) among 34 species (Fig. 6). These rearrangements included shuffling (genes moving to adjacent positions on the same strand without crossing PCGs), translocation (genes relocating across several genes, often involving PCGs), and inversion (genes switching strands) [56].

Compared to the ancestral Decapoda, within the family Hippolytidae, *L. anoplonyx* was found to have an additional *trnD* gene, and in *Saron marmoratus*, *trnC* translocated from downstream of *trnW* to downstream of *trnQ*. Within the family Pandalidae, *trnK* in *Plesionika izumiae* and *Plesionika lophotes* shuffled to downstream of *trnD*. Despite this, the gene arrangement in ten other sequenced species within the family Pandalidae (*Bitias brevis*, *Chlorotocus crassicornis*, *Heterocarpus sibogae*, *Heterocarpus ensifer*, *Pandalus borealis*, *Parapandalus sp.*, *Procletes levicarina*, *Plesionika edwardsii*, *Plesionika sindoi*, and *Plesionika ortmanni*) matched that of the ancestral pattern. Within the family Palaemonidae, most species of the genus *Palaemon* exhibited the *trnT* shuffling downstream of the *trnP*, with only *Palaemon modestus* maintaining a gene arrangement pattern consistent with the ancestor. There was a significant change in the gene arrangement of *Hymenocera picta*, where a gene fragment (*nad1-trnL1-16S rRNA-trnV-12S rRNA-trnI-trnQ*) was translocated from *trnS2* to downstream *nad4l*. Additionally, in *Ancylocaris brevicarpalis*, the *16S rRNA* shuffled downstream of *trnV* and underwent an inversion, while in *Anchistus australis*, the *trnL2* was lost, *trnL1* was shuffled downstream of *16S rRNA*, and *trnW* was translocated from downstream of *nad2* to downstream of *trnY*. The gene arrangement patterns of *Macrobrachium sp.* sequenced in this study and the remaining five species of Palaemonidae (*Palaemon modestus*, *Macrobrachium nipponense*, *Macrobrachium rosenbergii*, *Macrobrachium bullatum*, and *Macrobrachium lanchesteri*) matched those of the ancestor. In *Thor amboinensis* (Thoridae), extensive gene rearrangements were noted, including the reorganization of *trnQ*, *trnT*, and *nad6-cob-trnS2* into a new segment downstream of *trnS1*, and various other shuffles and translocations affecting *trnP*, *trnC*, *trnM*, *trnY*, along with inversions of *trnQ* and *trnI*. Within the Alpheidae family, *Synalpheus microneptunus* retains the ancestral gene arrangement. In contrast, nine other species—*Alpheus digitalis*, *Alpheus brevicristatus*, *Alpheus hoplocheles*, *Alpheus inopinatus*, *Alpheus japonicus*, *Alpheus bellulus*, *Alpheus lobidens*, *Alpheus randalli*, and *Leptalpheus forceps*—display a gene positional change. Specifically, *trnE* was translocated from downstream of *trnS1* to downstream of *cob*, accompanied by

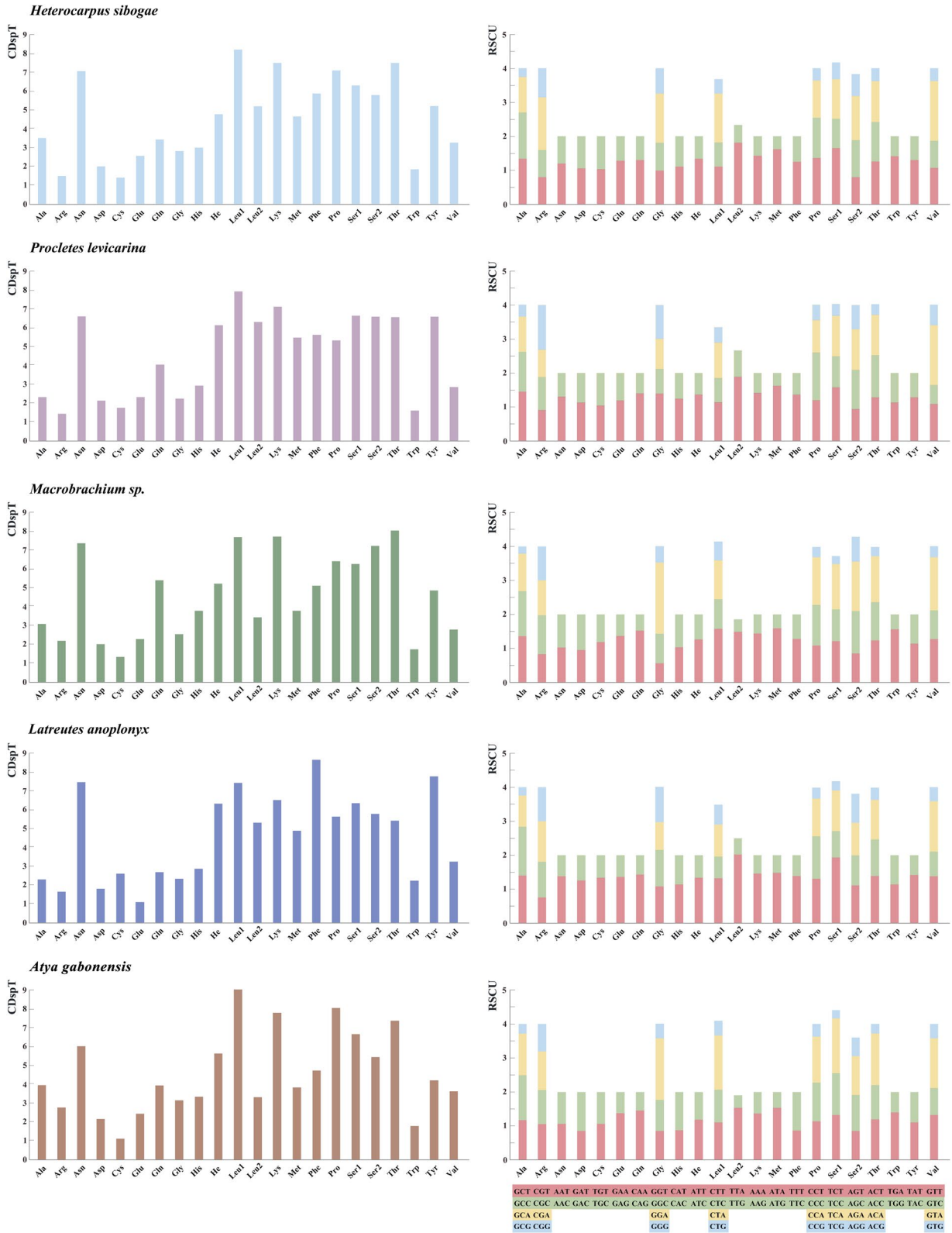

Fig. 3 The frequency of mitochondrial PCG amino acids (CDspT) and relative synonymous codon usage (RSCU) of five newly sequenced caridean mitogenomes

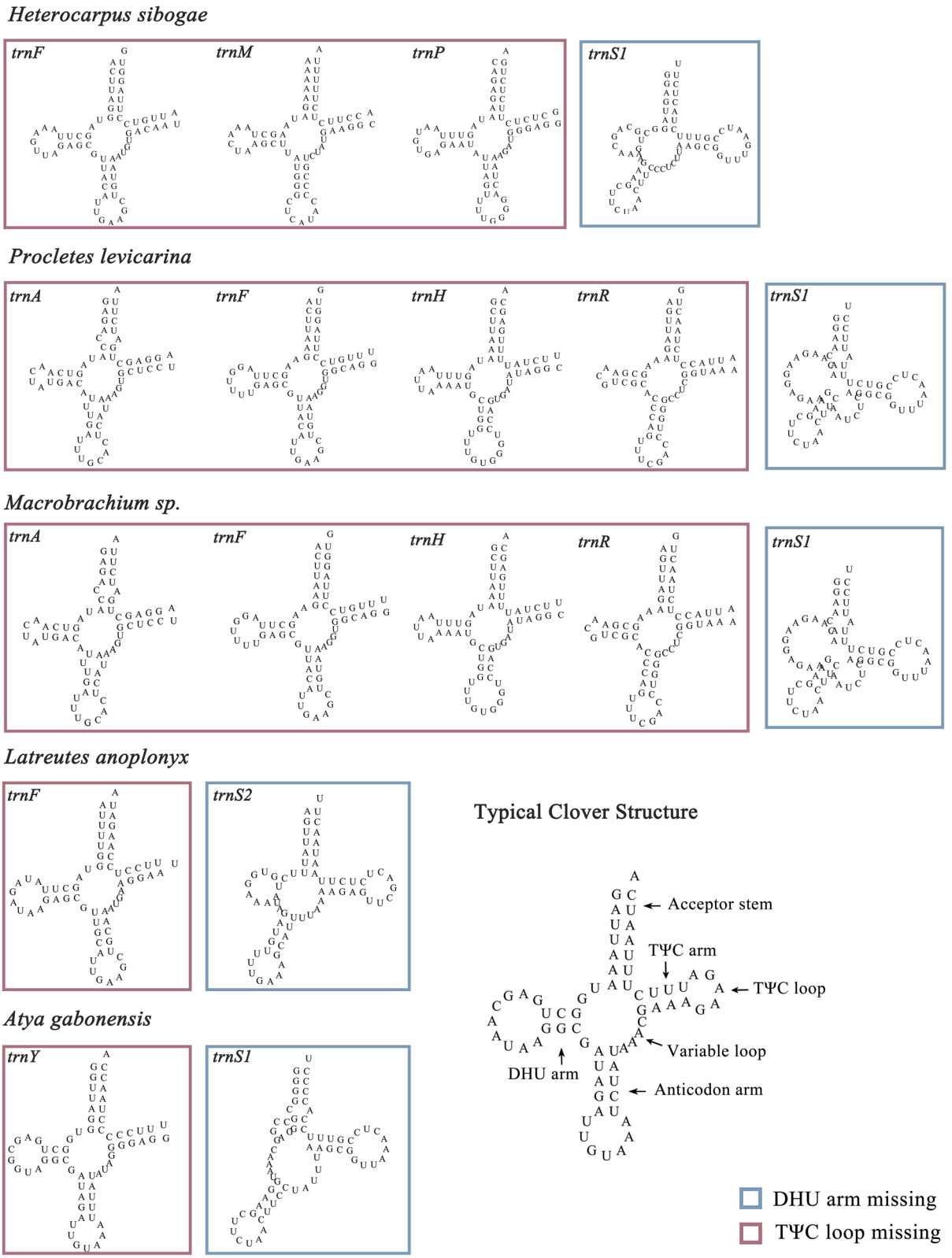

Fig. 4 Secondary structures of tRNAs of the five newly sequenced caridean mitogenomes

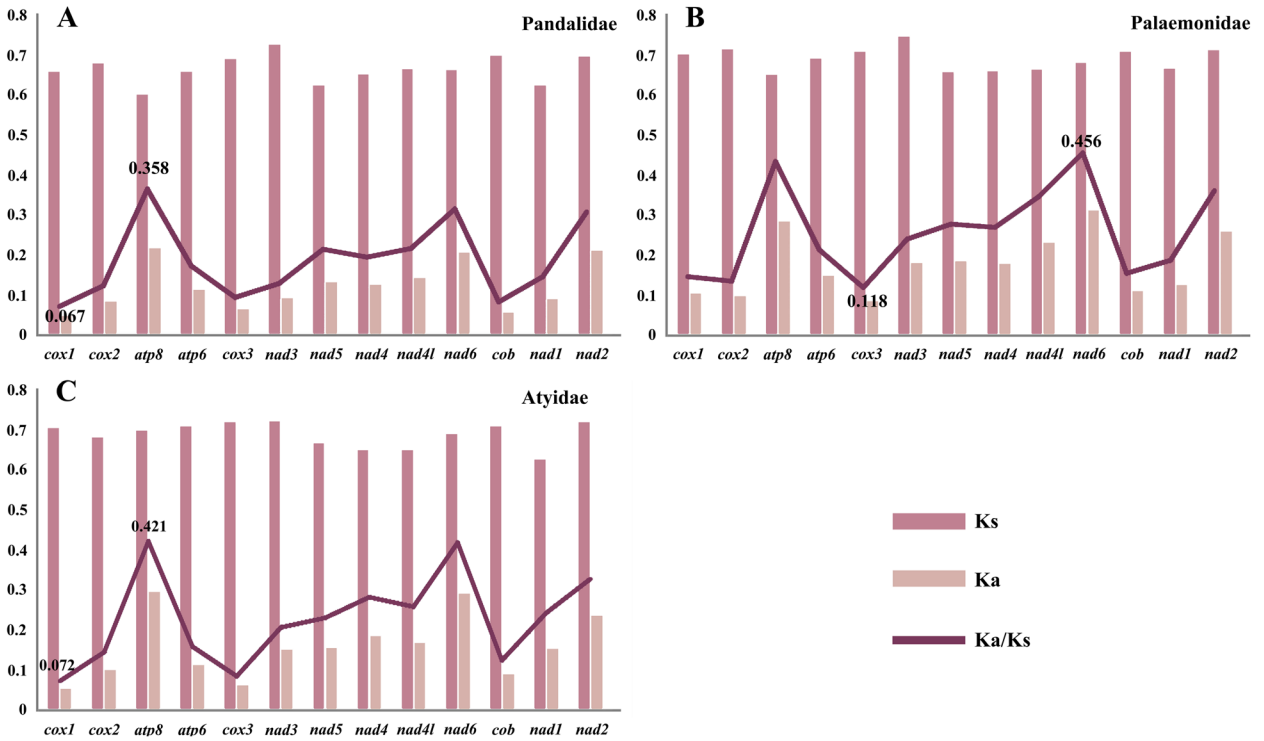

Fig. 5 The selective pressure analysis results for the 13 PCGs of species from three families are shown, with the species used for analysis listed in Table S1. **A** Result of Pandalidae. **B** Result of Palaemonidae. **C** Result of Atyidae

an inversion event. Noteworthy, *Alpheus lobidens* contains an extra *trnQ* gene. In the Lysmatidae family, *Exhippolysmata ensirostris* shows *trnL2* shuffled downstream of *cox2*, while *Lysmata vittata* has *trnA* shuffled downstream of *trnR*. The gene arrangements of the remaining four species, including *Lysmata amboinensis* and *Lysmata boggessi*, remain ancestral. In Rhynchocinetidae, *Rhynchocinetes durbanensis* and *Rhynchocinetes brucei* show *trnQ* shuffled downstream of *trnM*. Additionally, *R. durbanensis* has extra *trnI* and *trnM* genes, and in *R. brucei*, *trnD* has moved from downstream of *trnK* to downstream of *atp6*.

To date, four primary mechanisms or models have been proposed to explain mitochondrial gene rearrangements: tandem duplication and random loss [57], intramitochondrial recombination [58], tRNA miss-priming, and tandem duplication [59] and non-random loss [60]. Analysis of mitochondrial gene rearrangements in caridean shrimps shows that most patterns align with the tandem duplication and random loss model or the intramitochondrial recombination model. The tandem duplication and random loss model hypothesizes that errors during mitochondrial replication led to gene duplications, primarily generated by imprecise termination or slipped-strand mispairing. These duplications, followed by random gene loss due to natural selection, lead to gene rearrangements. Tandem duplication and random loss predominantly occur in Palaemonidae, Pandalidae, Lysmatidae, Hippolytidae, and Rhynchocinetidae. In *L. anoplonyx*, the ancestral gene cluster (*trnK-trnD*) was duplicated to form (*trnK-trnD*)-(*trnK-trnD*). Genomic parsimony makes it unlikely for two sets of functionally active genes to coexist, which likely led to the random loss of one set, resulting in the (*trnD-trnK-trnD*) cluster in *L. anoplonyx* (Fig. 6). Intramitochondrial recombination refers to rearrangements that occur when genes are reconnected following double-strand breaks. This process can result in long-distance gene movements and inversions, especially if breaks at multiple sites are not rejoined correctly. Recombination primarily occurs in Alpheidae and Thoridae. For instance, in all species of *Alpheus*, *trnE* undergoes long-distance movement accompanied by inversion, whereas in *Thor amboinensis* of Thoridae, multiple genes undergo long-distance movement, and some genes undergo inversion.

Phylogenetic relationships

Systematic phylogenetic analysis was conducted on two datasets (nucleotide sequences and amino acid sequences) of the 13 PCGs from 103 species across 13 families of Caridea. Two methods, ML and BI, were employed for the analysis. The BI and ML trees

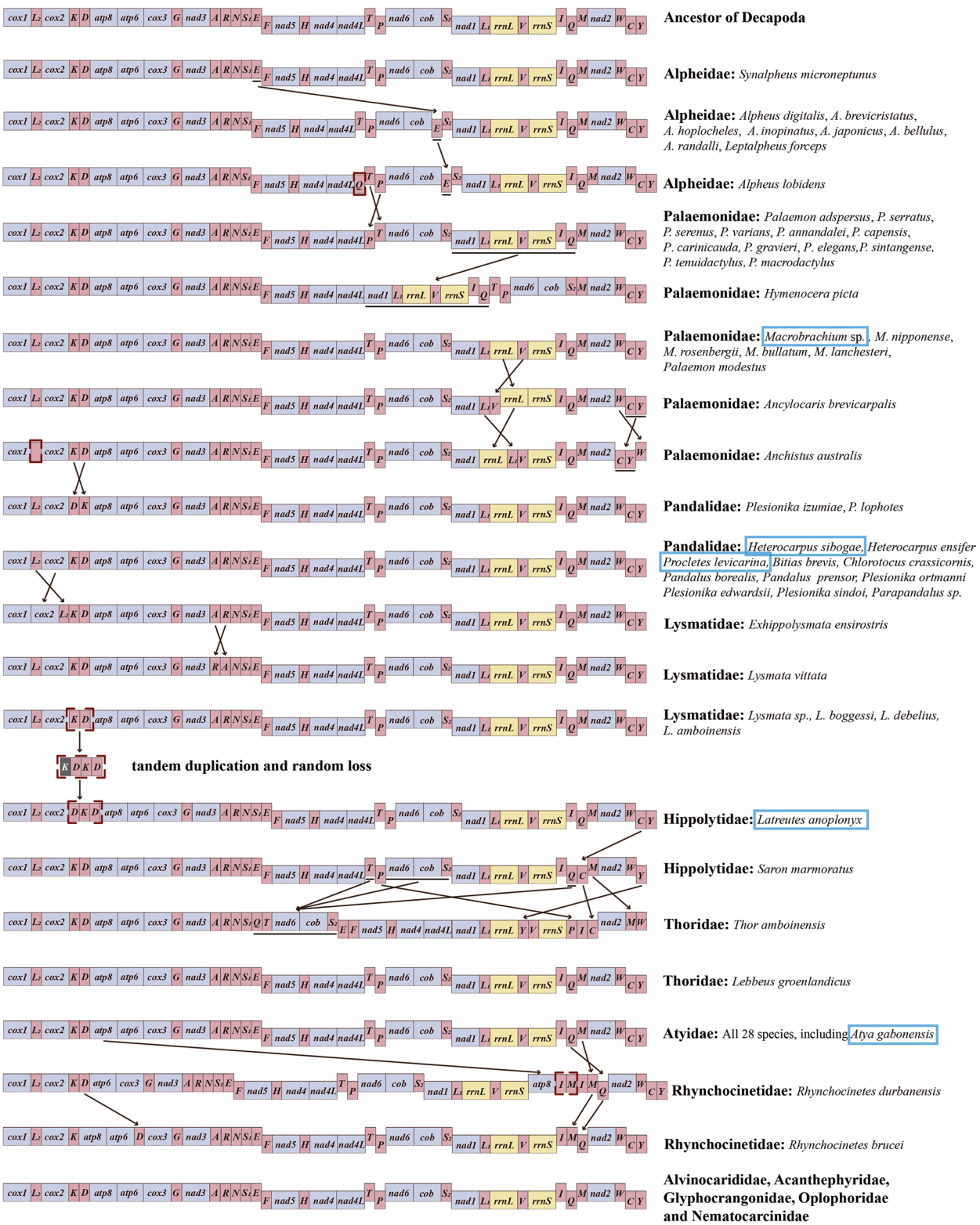

Fig. 6 Linear sequencing map of mitogenomes of Caridea, the five species in this study have been marked by blue box patterns. The tRNAs are labeled with amino acid abbreviations, and the lost genes are marked in dark gray

constructed using the two datasets exhibited slightly different topologies. Despite consistent topologies for most families, discrepancies arose in the relationships among Lysmatidae, Rhynchocinetidae, and Hippolytidae. Both analyses adopted the ML tree topology as the primary structure, integrating congruent branches from the ML and BI trees. Merged nodes displayed support values from both methods. The three families with differing BI results were analyzed separately. Results for PCGnt and PCGaa are presented in Figs. 7 and 8, respectively. Bayesian inference yielded high posterior probabilities, with most nodes showing strong support (values of 1). In contrast, the maximum likelihood analysis provided robust bootstrap support, although these values were generally lower than the posterior probabilities from the Bayesian inference, yet most nodes also exhibited high levels of support. Additionally, the phylogenetic results based on nucleotide sequences generally have higher support compared to those based on amino acid sequences.

The ML phylogenetic tree based on PCGnt sequences depicted the major lineages of Caridea as follows: ((Alpheidae + Palaemonidae) + (((Lysmatidae + Rhynchocinetidae) + Hippolytidae) + (Thoridae + Glyphocrangonidae))) + Pandalidae) + (Atyidae + ((Alvinocarididae + (Acanthephyridae + Oplophoridae)) + Nematocarcinidae))). The ML phylogenetic tree based on PCGaa sequences depicted the major lineages of Caridea as follows: ((((Alpheidae + Palaemonidae) + ((Atyidae + ((Alvinocarididae + (Acanthephyridae + Oplophoridae)) + Nematocarcinidae)) + Pandalidae)) + ((Thoridae + Glyphocrangonidae) + (Hippolytidae + Rhynchocinetidae))) + Lysmatidae). In both BI trees, the phylogenetic relationship of Lysmatidae, Rhynchocinetidae, and Hippolytidae was represented as Lysmatidae + (Rhynchocinetidae + Hippolytidae). Results showed that superfamilies like Palaemonoidea and Atyoidea were monophyletic, whereas Alpheoidea and Nematocarcinoidea were paraphyletic. At the family level, all Caridea families were monophyletic in the phylogenetic trees, although branching patterns slightly differed between the two datasets. In the nucleotide tree, all families were divided into two main clades. The first clade included eight families (BP = 99%; PP = 1.0): Alpheidae, Palaemonidae, Lysmatidae, Rhynchocinetidae, Hippolytidae, Thoridae, Glyphocrangonidae, and Pandalidae. The second clade consisted of five families (BP = 78%; PP = 0.69): Atyidae, Alvinocarididae, Acanthephyridae, Oplophoridae, and Nematocarcinidae. In the amino acid tree, Pandalidae clustered with the five families from the nucleotide tree's second clade, but this alignment was only supported in the BI tree (BP = 50%; PP = 1.0). Rhynchocinetidae, Hippolytidae, Thoridae, and Glyphocrangonidae still clustered together, with this branch again only supported in the BI tree (BP = 67%; PP = 1.0). The nucleotide-based ML tree indicated a close relationship between Hippolytidae and Lysmatidae/Rhynchocinetidae, forming a sister group (BP = 77%). In contrast, the ML tree based on amino acid sequences placed Lysmatidae as an independent clade at the terminal position of the tree (BP = 100%). Consistently, in the BI trees, Lysmatidae, Rhynchocinetidae, and Hippolytidae formed a sister group (PCGnt: PP = 1.0; PCGaa: PP = 0.85). Palaemonidae and Alpheidae showed the closest relationship, forming a sister group with high branch support in both datasets (PCGnt: BP = 100%; PP = 1.0; PCGaa: BP = 100%; PP = 0.85). Across all trees, Pandalidae and Atyidae consistently showed strong monophyly, with support values ranging from 99 to 100% in ML analyses and consistently 1.0 in BI analyses.

In both nucleotide and amino acid trees, within Pandalidae, *H. sibogae*, *H. ensifer*, and *Parapandalus sp*. formed a clade with perfect bootstrap and posterior probability support (PCGnt: BP = 100%; PP = 1.0, PCGaa: BP = 100%; PP = 1.0). In the nucleotide tree, these three species subsequently clustered with *P. levicarina* (BP = 81%; PP = 1.0), while in the amino acid tree, *P. levicarina* showed the closest affinity with *Chlorotocus crassicomis* before clustering with *Heterocarpus* species (BP = 91%; PP = 1.0). The division of five *Plesionika* species into two clades suggests polyphyly within *Plesionika* and *Heterocarpus*. Within the family Palaemonidae, both *Palaemon* and *Macrobrachium* showed strong monophyly. The sequenced *Macrobrachium sp.* in this study was closely related to *M. nipponense* and *M. bullatum* (PCGnt: BP = 97%; PP = 1.0, PCGaa: BP = 87%; PP = 1.0). In Atyidae, *A. gabonensis* and *Atyopsis moluccensis* formed a tight clade with strong support across both datasets (PCGnt: BP = 90%; PP = 0.99, PCGaa: BP = 100%; PP = 1.0).

Estimation of divergence times

The divergence of caridean species occurred in the Mesozoic Triassic around 206.91 million years ago (Mya). Subsequently, during the Mesozoic Jurassic, around 198.88 Mya and 191.01 Mya, they diverged into two main clades (Fig. 9 and Table 4). The divergence of families Palaemonidae and Alpheidae began in the Jurassic around 183.08 Mya. Subsequently, within the same period, Palaemonidae and Alpheidae differentiated further around 156.70 Mya and 151.81 Mya, respectively. The divergence of families Pandalidae and Atyidae also started in the Jurassic period, with the divergence time of Pandalidae being approximately 150.80 Mya, and that of Atyidae being around 166.42 Mya. Most Caridea families diverged during the Mesozoic Cretaceous, with notable times including Lysmatidae at 114.90 Mya, Rhynchocinetidae at 66.11

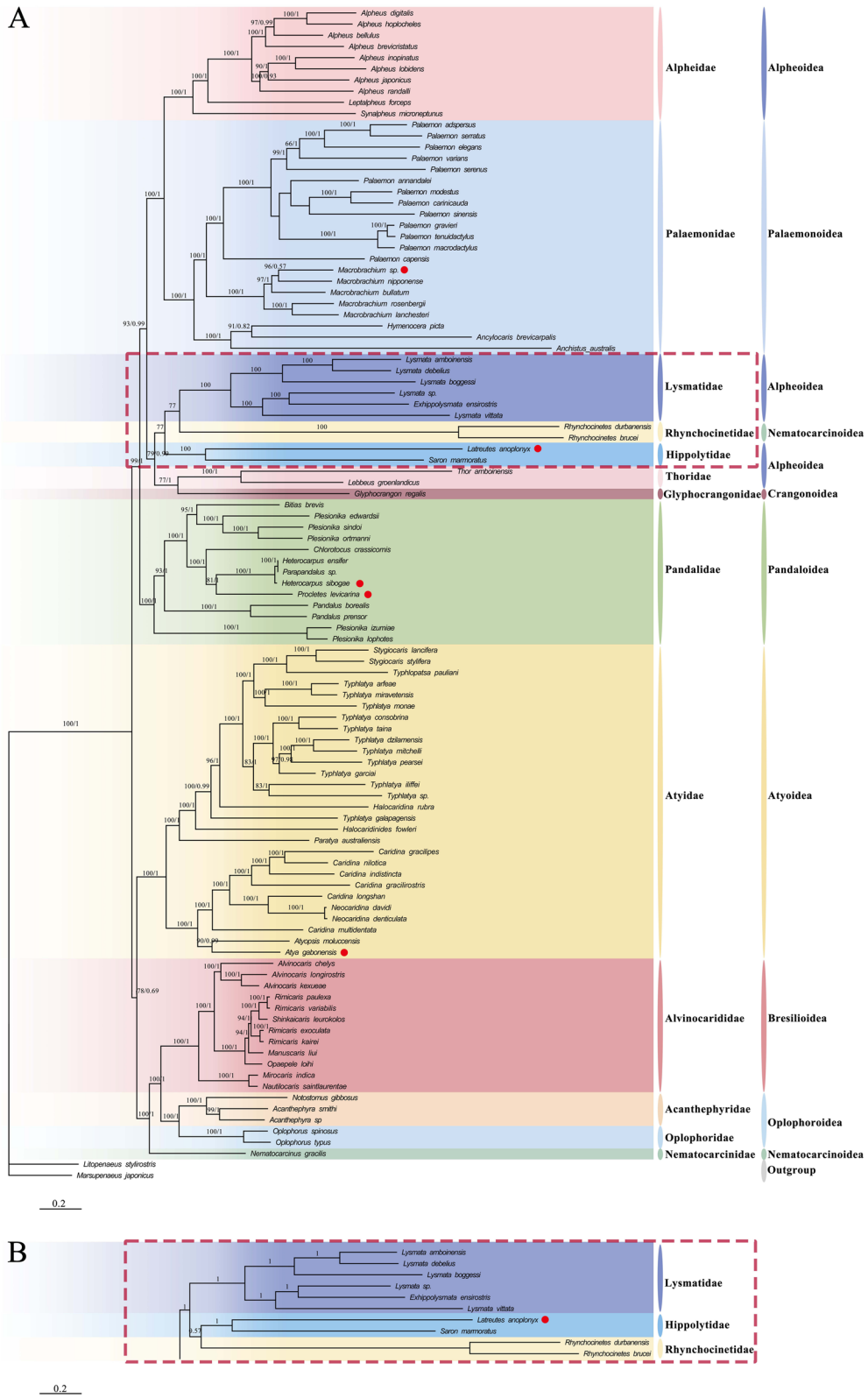

Fig. 7 Phylogenetic tree constructed based on nucleotide sequences of 13 PCGs of Caridea, the number in front of each node represents the support rate of ML/BI tree, and the five species in this study have been marked by red circular patterns. **A** shows the topological structure of the combined ML tree and BI tree, and the differences between BI and ML results are marked with red dashed boxes. **B** displays the different results in the BI tree

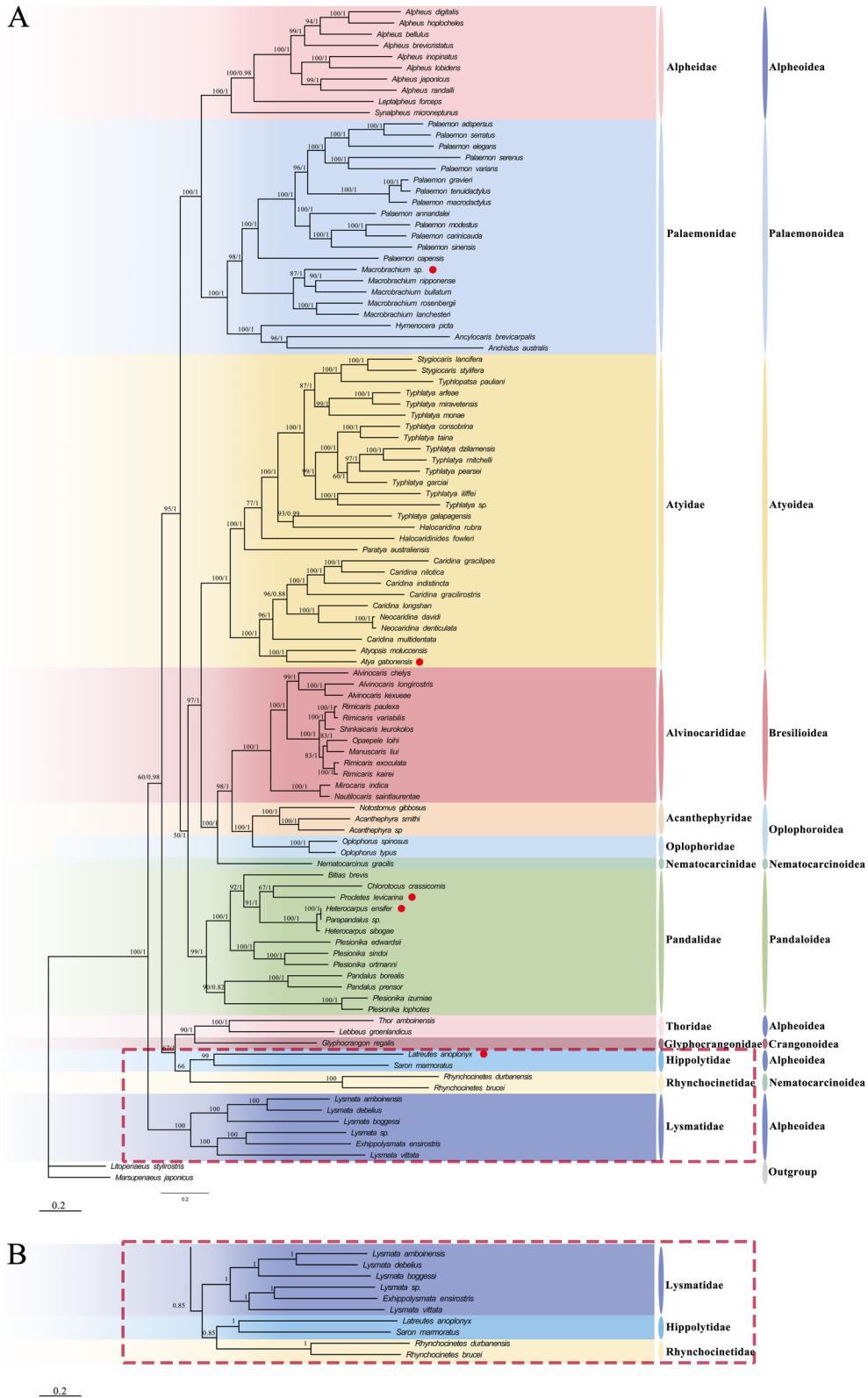

Fig. 8 Phylogenetic tree constructed based on amino acid sequences of 13 PCGs of Caridea, the number in front of each node represents the support rate of ML/BI tree, and the five species in this study have been marked by red circular patterns. **A** shows the topological structure of the combined ML tree and BI tree, and the differences between BI and ML results are marked with red dashed boxes. **B** displays the different results in the BI tree

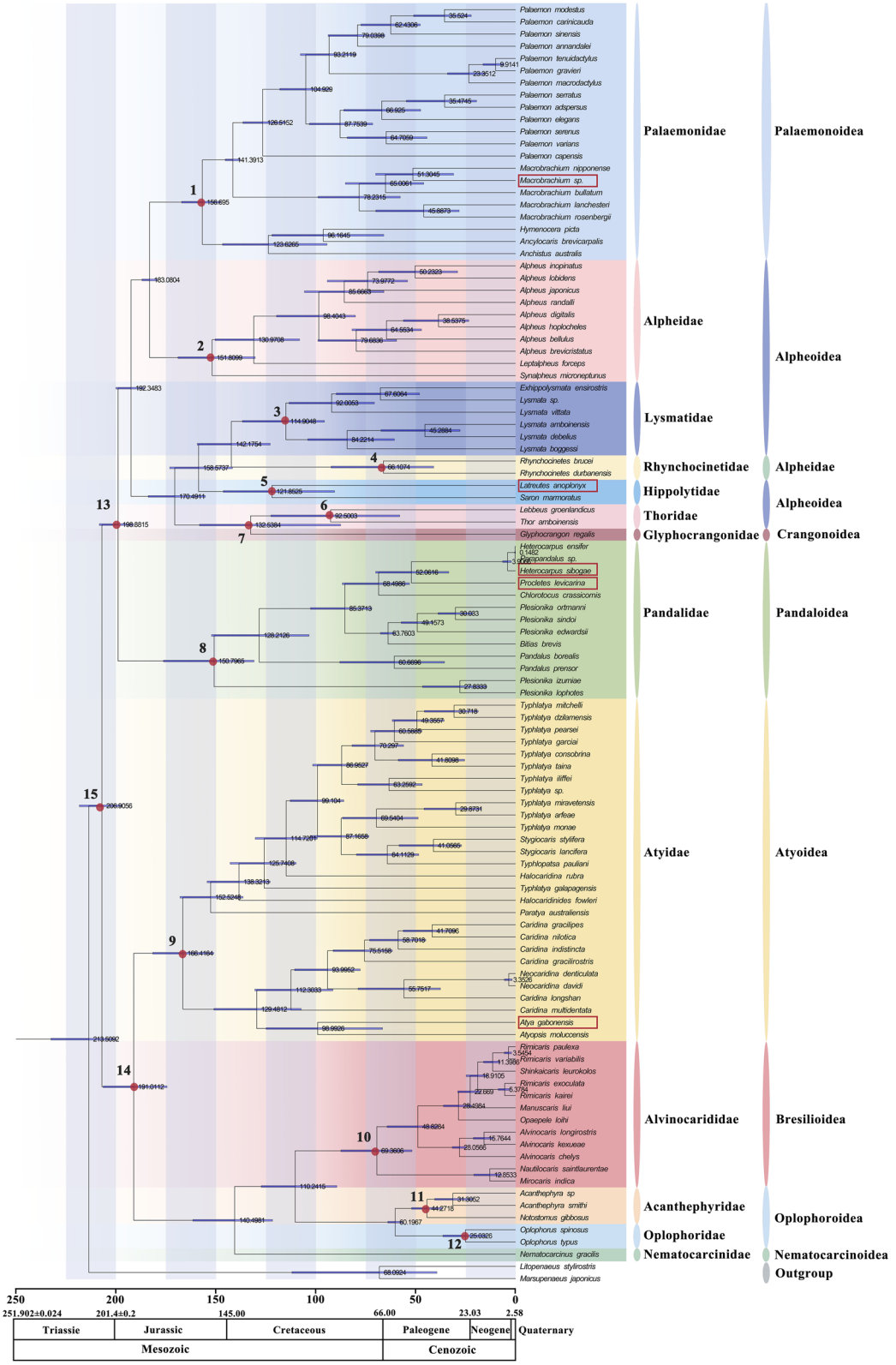

Fig. 9 Estimation of divergence time based on 13 PCGs of Caridea. The differentiation nodes of families within the Caridea are marked with red dots, and the five species in this study have been marked by red boxs

Table 4 Estimated divergence time of differentiation nodes among families of caridea

Node	Median (Mya)	95% Highest posterior density (HPD)
1	156.7	147.53 ~ 167.05
2	151.81	130.23 ~ 168.87
3	114.90	95.58 ~ 136.63
4	66.11	40.91 ~ 92.24
5	121.85	90.50 ~ 146.21
6	92.5	57.92 ~ 122.38
7	132.54	87.49 ~ 158.10
8	150.8	130.81 ~ 176.14
9	166.42	150.96 ~ 181.52
10	69.36	51.78 ~ 87.35
11	44.27	36.60 ~ 51.97
12	25.0326	14.37 ~ 36.26
13	198.88	191.03 ~ 208.26
14	191.01	174.34 ~ 206.29
15	209.91	196.82 ~ 218.24

Mya, and others as detailed. Acanthephyridae and Oplophoridae started diverging in the Cenozoic Paleogene, around 44.27 Mya and 25.03 Mya, respectively.

Within the family Pandalidae, this study sequenced *H. sibogae*, which diverged from *Parapandalus sp.* and *H. ensifer* in the early Cenozoic Neogene period, around 3.91 Mya. *P. levicarina* diverged from the genus *Heterocarpus* around 52.06 Mya in the Paleogene. Within the Palaemonidae family, a branch of the genus *Palaemon* began to diverge around 126.52 Mya in the Mesozoic Cretaceous period. Also, in Palaemonidae, *Macrobrachium* split from *Palaemon* around 141.39 Mya, with additional divergence noted around 78.23 Mya, both in the Cretaceous period. *Macrobrachium sp.* sequenced in this study diverged from *M. nipponense* around 51.30 Mya in the Paleogene. Within the family Atyidae, *A. gabonensis* diverged from *A. moluccensis* around 98.99 Mya in the Cretaceous period.

Discussion

The mitogenomes of five caridean species showed a higher proportion of AT bases compared to CG bases. Except for *L. anoplonyx*, the AT skew values were positive, a common phenomenon in mitogenome sequences of crustaceans [20, 21, 24]. Excluding the *cox1* gene of *L. anoplonyx*, which starts with CCG, the other mitogenomes typically begin with start codons ATA, ATG, ATT, ACG, and ATC. Some PCGs had incomplete stop codons, represented as T(AA) or TA(A), while the rest terminated with TAA and TAG as stop codons. This occurrence of incomplete stop codons is common in both vertebrate and invertebrate mitochondrial genomes [1, 20, 24, 61]. Analysis of amino acid content and codon usage frequency indicated differences among the five species. High-frequency codons included TTA (Leu), GTA (Val), GGA (Gly), ATA (Met), and TCT (Ser), while low-frequency codons consisted of TCG (Ser), GCG (Ala), CCG (Pro), and ACG (Thr). Additionally, in the tRNA structures of the five species, the *trnS1* genes in four species and the *trnS2* gene in *L. anoplonyx* lacked the DHU arm, preventing the formation of the typical cloverleaf structure. The phenomenon of *trnS* genes lacking the DHU arm has been reported in many studies of caridean mitogenomes [20, 62]. The selective pressure analysis of PCGs in Pandalidae, Palaemonidae, and Atyidae showed that the Ka/Ks values for all three families were less than 1, indicating purifying selection during evolution. Purifying selection on these PCGs highlights their crucial role in species survival and reproduction, necessitating conservation to prevent harmful mutations and maintain functional integrity. However, there were slight differences among the families. In Pandalidae and Atyidae, the gene under the highest selective pressure was *cox1*, while *atp8* was under the lowest. In Palaemonidae, *cox3* experienced the highest selective pressure, and *nad6* the lowest. Zhu et al. [63] also noted that *nad6* in *Palaemon* and *Macrobrachium* (Palaemonidae) was under the least selective pressure.

Gene rearrangement was uncommon in sequenced caridean mitogenomes, with only one-third showing such changes. A total of 14 gene rearrangement patterns were identified. Comparative analysis revealed three main types of gene rearrangements in caridean mitogenomes: shuffling, translocation, and inversion, with shuffling and translocation most prevalent. Among the five newly sequenced species, only *L. anoplonyx* exhibited gene duplication, while the gene arrangements of the remaining four species were consistent with those of the ancestor. Additionally, a novel gene rearrangement pattern was discovered in the family Hippolytidae. Diverse gene rearrangement patterns were observed across seven caridean families, including Pandalidae, Palaemonidae, Hippolytidae, Thoridae, Alpheidae, Lysmatidae, and Rhynchocinetidae. Some genera have already displayed unique gene arrangement patterns, such as *Alpheus* in the family Alpheidae, where all species exhibited the same positional change in the *trnE* gene compared to the ancestral sequence. Similarly, within *Palaemon* in the family Palaemonidae, except for *P. modestus*, all species showed an interchange of the *trnP* and *trnT* genes' positions. The study suggests that these rearrangement patterns can be explained by the tandem duplication and

random loss model, along with the intramitochondrial recombination model.

Earlier phylogenetic studies have suggested using mitochondrial gene arrangements as novel molecular markers for analysis [56]. Several studies have already revealed certain regularities between mitochondrial gene arrangement and phylogenetic relationships [64, 65]. This approach has potential for estimating phylogenetic relationships across arthropods [23, 66]. In Caridea, a combined analysis of mitochondrial gene arrangements and phylogeny divided all families into two major clades in the nucleotide tree. One clade included five families, Atyidae, Alvinocarididae, Acanthephyridae, Oplophoridae, and Nematocarcinidae, none of which had experienced gene rearrangement. The second clade included seven families known for gene rearrangements, although Glyphocrangonidae, also part of this clade, did not show such changes. In the amino acid tree, these five families also grouped together at the core of the tree. The seven families with gene rearrangement and Glyphocrangonidae formed other branches. Limited data on Glyphocrangonidae (only one species) renders its phylogenetic position uncertain. This uncertainty might result from long-branch attraction, which suggests a potential link between gene rearrangement and overall phylogeny. In the nucleotide tree, families with conserved gene order and those with rearranged gene order were distinctly divided into two clades. In the amino acid tree, Pandalidae, with just two rearranged species, was most closely related to the five families without rearrangements. In the nucleotide tree, Pandalidae, having the fewest rearranged species, was located at the periphery of the clade containing families with gene rearrangements. Alpheidae and Palaemonidae, having the most rearranged species, formed sister groups. Further analysis showed that *Alpheus* species within Alpheidae, sharing a common rearrangement pattern, clustered with *L. forceps* in both datasets. Meanwhile, *S. microneptunus*, which had not undergone rearrangement, was located at the outermost branches of this family. In Palaemonidae, the genus *Macrobrachium* without gene rearrangement formed a separate clade, whereas three species (*H. picta*, *A. brevicarpalis*, *A. australis*) with different rearrangements clustered together. In Pandalidae, two *Plesionika* species with gene rearrangement formed a clade, while three *Plesionika* species without rearrangement formed another clade. Additionally, in the nucleotide tree, Pandalidae species with conserved gene order grouped together, with two rearranged species on the family's outermost branches.

The phylogenetic relationships within Caridea have been a key research focus, evolving significantly as more Caridea mitogenomes are sequenced. The results of this study indicated that all families within Caridea were monophyletic. Although the phylogenetic analyses based on nucleotide sequences and amino acid sequences yielded slightly different results, the relationships among most families were consistently resolved. For example, Alpheidae and Palaemonidae were sister taxa, a relationship supported by numerous studies [1, 20, 21, 24]. Similarly, Hippolytidae, Lysmatidae, and Rhynchocinetidae were identified as sister taxa, though there were minor discrepancies with findings from Kong et al. [1] and Cronin et al. [26] using 13 PCGs. While Kong et al. [1] identified Hippolytidae, Rhynchocinetidae, and Thoridae as closely related, followed by Lysmatidae, our findings suggest Thoridae is closer to Glyphocrangonidae. Cronin et al. [26] supported the relationship between Hippolytidae and Lysmatidae, but their results placed Rhynchocinetidae as the outermost branch in the phylogenetic tree. These differences may stem from variations in species richness used for phylogenetic analysis. Both Pandalidae and Atyidae exhibited strong monophyly, consistent with previous research [20, 24]. Initially, some studies suggested Atyidae as the basal lineage of Caridea [18]; however, including more species has refuted this, a finding our study supports [20]. Alvinocarididae, Acanthephyridae, and Oplophoridae formed sister taxa, in agreement with Chak et al. [27] and Cronin et al. [26], with Nematocarcinidae and Atyidae following closely. Five *Plesionika* species split into two clades, with *Parapandalus sp.* nested within *Heterocarpus*, demonstrating their polyphyly as noted in studies by Wang et al. [14] and Liao et al. [22]. However, it differs from Kong et al. [1], who considered *Heterocarpus* to be a monophyletic group. Additionally, several studies based on partial mitochondrial sequences (*cox1* and *16S rRNA*) also supported the polyphyly of *Plesionika* [67, 68]. Chow et al. [3] used a combination of four nuclear genes and three rRNA genes to analyze more Palaemonidae species, suggesting that *Macrobrachium* is polyphyletic. In conclusion, varying tree-building methods and gene sequences can lead to differing phylogenetic results. The taxonomic status of some families within Caridea remains subject to change, thus further research is needed to clarify the phylogenetic positions of the various families within Caridea.

Divergence time analysis indicates that Caridea diverged around 206.91 Mya during the Mesozoic Triassic period, aligning with estimates by Sun et al. [61]. The Triassic period marks the beginning of the Mesozoic Era and a time of profound transformation in marine ecosystems. Following the Permian-Triassic Mass Extinction (PTME), many ancient marine taxa vanished at the start of the Triassic, making way for new groups like malacostracan crustaceans, including crabs and shrimps [69, 70]. The Mesozoic Marine Revolution (MMR) began in the Middle

and Late Triassic, during which marine life underwent rapid diversification and radiation [70]. Additionally, the Carnian Pluvial Episode (CPE), a major climatic shift in the Late Triassic, likely had a significant impact on marine evolution [71, 72]. The Carnian Pluvial Episode was marked by repeated volcanic eruptions from the Wrangellia Large Igneous Province, causing global warming, acid rain, soil erosion, ocean acidification, and seafloor anoxia [72, 73]. This period saw the emergence of the first scleractinian reefs and rock-forming calcareous nannofossils in the ocean [72]. Consequently, the new predator groups that originated after the PTME, including decapod crustaceans, began to diversify significantly [70]. Subsequently, Caridea split into two major lineages during the Jurassic, likely influenced by the breakup of the supercontinent Pangea. The breakup of the supercontinent Pangea gave rise to the expansion of the Neo-Tethys and the Central Atlantic oceans, accompanied by intense volcanic activity. This led to a globally warmer and more humid climate. Favorable sea temperatures and nutrient-rich waters brought about by upwelling currents fostered the flourishing of marine life [74]. Concurrently, the rifting of Pangea resulted in the gradual opening of the Tethys Sea, which became a major marine gateway connecting the eastern and western hemispheres. This facilitated both marine species migration and biodiversity increase [75]. Sun et al. estimated Alvinocarididae divergence at about 61.39 Mya during the Mesozoic Cretaceous, close to our estimate of 66.36 Mya, with a broad HPD interval. However, their estimation for Thoridae divergence at 20.09 Mya during the Neogene contrasts sharply with our estimate of 92.50 Mya during the Cretaceous. Zhu et al. [11] estimated Palaemonidae divergence at 226.98 Mya in the Triassic, differing from our estimate of about 156.7 Mya in the Jurassic. Sun et al.'s estimates align more closely with ours. [61]. This study's estimate for Atyidae divergence at about 166.42 Mya during the Jurassic aligns closely with Sun et al.'s but contrasts sharply with Zhu et al.'s 231.91 Mya and von Rintelen's 345 Mya estimations [76]. However, Zhu et al. estimated the divergence time of Alpheus genus to be around 127.44 Mya (with a range of 81.81 to 188.02 Mya), which is relatively close to this study's estimation of 98.40 Mya. Overall, it appears that most families of Caridea underwent divergence during the Mesozoic Cretaceous period. Numerous significant geological events occurred during the Cretaceous period, such as extensive volcanic activities [77], oceanic anoxic events [78, 79], and major radiations and turnovers of biodiversity [80]. These events led to environmental changes and the reallocation of ecological niches, which likely facilitated the diversification of most families within the suborder Caridea. We conducted molecular divergence estimations for all verified Caridea species in GenBank, finding general consistency with previous studies. Discrepancies may arise from variations in sequence data selection, fossil calibration settings, and the placement of these calibrations in molecular clocks.

Conclusion

This study obtained complete mitogenome sequences for five caridean species, enhancing the GenBank database's collection of Pandalidae, Palaemonidae, Hippolytidae, and Atyidae mitogenomes. Analysis of the basic structure and characteristics of these five mitogenomes revealed that their genomic structure compositions were generally similar. Except for *L. anoplonyx* encoding 38 genes, the other four species encoded 37 genes each. The AT base content of all five mitogenomes was generally higher than the CG base content. There were differences in codon usage preferences among different species. The analysis of selective pressure in Pandalidae, Palaemonidae, and Atyidae showed that the Ka/Ks values of PCGs in all three families are less than 1, indicating that purifying selection acts on their evolution, but there are slight differences among different families. Comparison of ancestral gene arrangements with those of 103 sequenced caridean species revealed gene rearrangements in 34 species, encompassing 14 distinct patterns. The phylogenetic analysis results indicated that each Caridea family formed a monophyletic group, where Palaemonidae and Alpheidae emerged as sister taxa. Glyphocrangonidae and Thoridae species exhibited the closest phylogenetic relationship. Both Pandalidae and Atyidae demonstrated robust monophyly. Hippolytidae, Lysmatidae, and Rhynchocinetidae were identified as sister groups. The study substantiated the genetic diversity within *Plesionika* and *Heterocarpus*. A correlation between Caridea phylogeny and mitochondrial gene arrangement was revealed through combined analysis. However, to validate this finding, additional mitogenomes from diverse species are imperative in the future. Gene arrangement may prove to be a valuable molecular marker for estimating arthropod phylogenetic relationships. Using fossil records from TimeTree, divergence times were estimated, showing Caridea species first diverged during the Mesozoic Triassic and then split into two main lineages during the Mesozoic Jurassic. Additionally, most Caridea families diverged during the Mesozoic Cretaceous.

Supplementary Information

The online version contains supplementary material available at https://doi.org/10.1186/s12864-024-10775-4.

Supplementary Material 1.

Authors' contributions
SYM and LWT wrote and reviewed the manuscript. CJ revised the manuscript. LJJ Investigation. YYY revised the manuscript and designed the research project. XKD funding acquisition. All authors reviewed the manuscript.

Funding
The present manuscript was financially supported by the Project of Bureau of Science and Technology of Zhoushan (No. 2021C21017) and the National Key R&D Program of China (2019YFD0901204).

Availability of data and materials
All mitogenome sequences data were deposited in Genbank with accession number OP380621 (Heterocarpus sibogae) (https://www.ncbi.nlm.nih.gov/nuccore/OP380621), OR120370 (Procletes levicarina) (https://www.ncbi.nlm.nih.gov/nuccore/OR120370), OQ512153 (Macrobrachium sp.) (https://www.ncbi.nlm.nih.gov/nuccore/OQ512153), OR120369 (Latreutes anoplonyx) (https://www.ncbi.nlm.nih.gov/nuccore/OR120369) and OP650929 (Atya gabonensis) (https://www.ncbi.nlm.nih.gov/nuccore/OP650929). The raw mitogenome sequencing datasets of five caridean species have been submitted to the NCBI SRA with the following accession numbers: SRX24926934 (H. sibogae), SRX24926936 (P. levicarina), SRX24926938 (Macrobrachium sp.), SRX24926937 (L. anoplonyx), SRX24926935 (A. gabonensis), and are available online at https://www.ncbi.nlm.nih.gov/sra/?term=PRJNA1123500.

Declarations

Ethics approval and consent to participate
The caridean sample collection is strictly under the framework of law in China. The protocol was approved by the National Engineering Centre of Zhejiang Ocean University and all experimental procedures were carried out in accordance with institutional guidelines for the care and use of laboratory animals.

Consent for publication
Not applicable.

Competing interests
The authors declare no competing interests.

Author details
[1]National Engineering Research Center for Marine Aquaculture, Zhejiang Ocean University, Lincheng Street, Zhoushan, Zhejiang Province 316022, China. [2]Jiangsu Coastal Area Institute of Agricultural Science, Yancheng, Jiangsu Province, China. [3]Key Laboratory of Sustainable Utilization of Technology Research for Fisheries Resources of Zhejiang Province, Scientific Observing and Experimental Station of Fishery Resources for Key Fishing Grounds, Ministry of Agriculture and Rural Affairs of China, Zhejiang Marine Fisheries Research Institute, Lincheng Street, Zhoushan, Zhejiang Province 316022, China.

Received: 11 May 2024 Accepted: 4 September 2024
Published online: 16 October 2024

References

1. Kong D, Gan Z, Li X. Phylogenetic relationships and adaptation in deep–sea carideans revealed by mitogenomes. Gene. 2024;896:148054.
2. Kumaralingam S, Raghunathan C. An account of some reef associated caridean shrimps and stomatopods of Andaman Islands. Rec Zool Surv India. 2016;116(2):117–28.
3. Chow LH, De Grave S, Tsang LM. The family Anchistioididae Borradaile, 1915 (Decapoda: Caridea) is a synonym of Palaemonidae Rafinesque, 1815 based on molecular and morphological evidence. J Crustacean Biol. 2020;40(3):277–87.
4. Knowlton N. Sexual selection and dimorphism in two demes of a symbiotic, pair-bonding snapping shrimp. Evolution. 1980;34(1):161–73.
5. Knowlton N, Keller BD. A New, Sibling species of snapping shrimp associated with the caribbean sea anemone bartholomea annulata. B Mar Sci. 1983;33(2):353–62.
6. Pratchett MS. Influence of coral symbionts on feeding preferences of prown-of-thorns starfish acanthaster planci in the western pacific. Mar Ecol Prog Ser. 2001;214:111–9.
7. Duffy JE. The ecology and evolution of eusociality in sponge-dwelling Shrimp. Genes Behav Evol Soc Insects. 2003:1–38.
8. Silliman BR, Layman CA, Altieri AH. Symbiosis between an Alpheid Shrimp and a xanthoid crab in salt marshes of mid-atlantic states, U.S.A. J Crustac Biol. 2003;23(4):876–9.
9. Bauer RT. Remarkable shrimps-adaptations and natural history of the carideans. Norman, Minnesota : University of Oklahoma Press; 2004.
10. Stimpson W. Prodromus descriptionis animalium evertebratorum, quae in Expeditione ad Oceanum Pacificum Septentrionalem, a Republica Federata missa, Cadwaladaro Ringgold et Johanne Rodgers Ducibus, observavit et descripsit. Proc Acad Nat Sci Phila. 1858;10:93–110.
11. Zhu L. Species identification and mitochondrial genome structure and phylogenetic analysis of two marine ornamental shrimp. Zhoushan, China: Zhejiang Ocean University; 2021.
12. Li X, Liu R, Liang X. FAUNA SINICA: Invertebrata. Crustacea, Decapoda, Palaemonoidea. Beijing: Science Press; 2007;44.
13. Li X, Liu R, Liang X. FAUNA SINICA: Invertebrata. Crustacea, Decapoda, Atyidae. Beijing: Science Press; 2004;36.
14. Wang Y, Ma KY, Tang LM, Wakabayashi K, Chan TY, De Grave S, et al. Confirming the systematic position of two enigmatic shrimps, *Amphionides* and Procaridida (Crustacea: Decapoda). Zool Scr. 2021;50(6):812–23.
15. Miller AD, Murphy NP, Burridge CP, Austin CM. Complete mitochondrial DNA sequences of the decapod crustaceans *Pseudocarcinus gigas* (Menippidae) and *Macrobrachium rosenbergii* (Palaemonidae). Mar Biotechnol. 2005;7:339–49.
16. Short JW, Humphrey CL, Page TJ. Systematic revision and reappraisal of the Kakaducarididae Bruce (Crustacea : Decapoda : Caridea) with the description of three new species of *Leptopalaemon* Bruce & Short. Invertebr Syst. 2013;27(1):87–117.
17. De Grave S, Fransen CH, Page TJ. Let's be pals again: major systematic changes in Palaemonidae (Crustacea: Decapoda). PeerJ. 2015;3:e1167.
18. Bracken HD, De Grave S, Toon A, Felder DL, Crandall KA. Phylogenetic position, systematic status, and divergence time of the Procarididea (Crustacea: Decapoda). Zool Scr. 2010;39(2):198–212.
19. Li CP, De Grave S, Chan TY, Lei HC, Chu KH. Molecular systematics of caridean shrimps based on five nuclear genes: Implications for superfamily classification. Zool Anz. 2011;250(4):270–9.
20. Ye YY, Miao J, Guo YH, Gong L, Jiang LH, Lü ZM, et al. The first mitochondrial genome of the genus *Exhippolysmata* (Decapoda: Caridea: Lysmatidae), with gene rearrangements and phylogenetic associations in Caridea. Sci Rep-UK. 2021;11(1):1–13.
21. Sun S, Cheng J, Sun S, Sha Z. Complete mitochondrial genomes of two deep–sea pandalid shrimps, *Heterocarpus ensifer* and *Bitias brevis*: insights into the phylogenetic position of Pandalidae (Decapoda: Caridea). J Oceanol Limnol. 2020;38(3):816–25.
22. Liao Y, Ma KY, De Grave S, Komai T, Chan TY, Chu KH. Systematic analysis of the caridean shrimp superfamily Pandaloidea (Crustacea: Decapoda) based on molecular and morphological evidence. Mol Phylogenet Evol. 2019;134:200–10.
23. Tan MH, Gan HM, Lee YP, Poore GC, Austin CM. Digging deeper: new gene order rearrangements and distinct patterns of codons usage in mitochondrial genomes among shrimps from the Axiidea, Gebiidea and Caridea (Crustacea: Decapoda). PeerJ. 2017;5:e2982.
24. Wang Q, Wang Z, Tang D, Xu X, Tao Y, Ji C, et al. Characterization and comparison of the mitochondrial genomes from two Alpheidae species and insights into the phylogeny of Caridea. Genomics. 2020;112(1):65–70.
25. Liu H. Sequence and phylogenetic analysis of the mitochondrial genome for a giant clam commensal shrimp *Anchistus australis* (Decapoda: Caridea: Palaemonidae). Mitochondrial DNA B Resour. 2019;5(1):312–3.
26 Cronin TJ, Jones SJM, Baeza JA. The complete mitochondrial genome of the spot prawn, Pandalus platyceros Brandt in von Middendorf, 1851 (Decapoda: Caridea: Pandalidae), assembled from linked-reads sequencing. J Crustac Biol. 2022;42(1):ruac003.
27 Chak STC, Barden P, Baeza JA. The complete mitochondrial genome of the eusocial sponge-dwelling snapping shrimp Synalpheus microneptunus. Sci Rep-UK. 2020;10(1):7744.

28. Xing J. The types of molecular markers and the researchch and applications of molecular markers technoloyy on the aquatic creature. Chin J Fish. 2002;15(01):61–70.
29. Elmerot C, Arnason U, Gojobori T, Janke A. The mitochondrial genome of the pufferfish, Fugu rubripes, and ordinal teleostean relationships. Gene. 2002;295(2):163–72.
30. Xiao L. Mitochondrial genome evolution in Metazoa: origin, size, and gene arrangement. Lett Biotechnol. 2010;21(05):721–6.
31. Shen X. Mitochondrial genomic characters of malacostracans and sipunculansand the molecular evolutionary research based on mitochondrial genomes. Qingdao: Chinese Academy of Sciences; 2008.
32. Boore JL, Brown WM. Big trees from little genomes: mitochondrial gene order as a phylogenetic tool. Curr Opin Genet Dev. 1998;8(6):668–74.
33. Dong J. Zhejiang Fauna: Crustaceans. Hangzhou, China: Zhejiang Science and Technology Press; 1991.
34. Aljanabi SM, Martinez I. Universal and rapid salt-extraction of high quality genomic DNA for PCR–based techniques. Nucleic Acids Res. 1997;25(22):4692–3.
35. Torkian B, Hann S, Preisner E, Norman RS. BLAST-QC: automated analysis of BLAST results. Environ microbiome. 2020;15(1):15.
36. Jin JJ, Yu WB, Yang JB, Song Y, DePamphilis CW, Yi TS, et al. GetOrganelle: a fast and versatile toolkit for accurate de novo assembly of organelle genomes. Genome Biol. 2020;21(1):241.
37. Walker BJ, Abeel T, Shea T, Priest M, Abouelliel A, Sakthikumar S, et al. Pilon: an integrated tool for comprehensive microbial variant detection and genome assembly improvement. PLoS One. 2014;9(11):e112963.
38. Bernt M, Donath A, Jühling F, Externbrink F, Florentz C, Fritzsch G, et al. MITOS: improved de novo metazoan mitochondrial genome annotation. Mol Phylogenet Evol. 2013;69(2):313–9.
39. Weber C, Hirst MB, Ernest B, Schaub NJ, Wilson KM, Wang K, et al. SEQUIN is an R/Shiny framework for rapid and reproducible analysis of RNA-seq data. Cell rep methods. 2023;3(3):100420.
40. Kumar S, Stecher G, Li M, Knyaz C, Tamura K. MEGA X: molecular evolutionary genetics analysis across computing platforms. Mol Biol Evol. 2018;35(6):1547–9.
41. Hassanin A, Léger N, Deutsch J. Evidence for multiple reversals of asymmetric mutational constraints during the evolution of the mitochondrial genome of metazoa, and consequences for phylogenetic inferences. Syst Biol. 2005;54(2):277–98.
42. Benson G. Tandem repeats finder: a program to analyze DNA sequences. Nucleic Acids Res. 1999;27(2):573–80.
43. Xia X. DAMBE7: New and improved tools for data analysis in molecular biology and evolution. Mol Biol Evol. 2018;35(6):1550–2.
44. Rozas J, Ferrer-Mata A, Sánchez-DelBarrio JC, Guirao-Rico S, Librado P, Ramos-Onsins SE, et al. DnaSP 6: DNA sequence polymorphism analysis of large data sets. Mol Biol Evol. 2017;34(12):3299–302.
45. Zhang D, Gao F, Jakovlić I, Zou H, Zhang J, Li WX, et al. PhyloSuite: an integrated and scalable desktop platform for streamlined molecular sequence data management and evolutionary phylogenetics studies. Mol Ecol Resour. 2020;20(1):348–55.
46. Castresana J. Selection of conserved blocks from multiple alignments for their use in phylogenetic analysis. Mol Biol Evol. 2000;17(4):540–52.
47. Minh BQ, Schmidt HA, Chernomor O, Schrempf D, Woodhams MD, Von Haeseler A, et al. IQ-TREE 2: new models and efficient methods for phylogenetic inference in the genomic era. Mol Biol Evol. 2020;37(5):1530–4.
48 Ronquist F, Teslenko M, Van Der Mark P, Ayres DL, Darling A, Höhna S, et al. MrBayes 3.2: efficient Bayesian phylogenetic inference and model choice across a large model space. Syst Biol. 2012;61(3):539–42.
49. Swofford DL. PAUP, phylogenetic analysis using parsimony, version 3.1. Champagne Urbana: Natural HistorySuvey; 1993.
50. Darriba D, Posada D, Kozlov AM, Stamatakis A, Morel B, Flouri T. ModelTest-NG: a new and scalable tool for the selection of DNA and protein evolutionary models. Mol Biol Evol. 2020;37(1):291–4.
51. Nylander JAA. MrModeltest version 2. Program distributed by the author: Evolutionary Biology Centre, Uppsala University, Uppsala, Sweden; 2004.
52. Kalyaanamoorthy S, Minh BQ, Wong TKF, Von Haeseler A, Jermiin LS. ModelFinder: fast model selection for accurate phylogenetic estimates. Nat Methods. 2017;14(6):587–9.
53. FigTree, Version 1.4.3. Available online: http://tree.bio.ed.ac.uk/software/figtree/. Accessed 1 Jul 2016.
54 Drummond AJ, Suchard MA, Xie D, Rambaut A. Bayesian phylogenetics with BEAUti and the BEAST 1.7. Mol Biol Evol. 2012;29(8):1969–73.
55 Rambaut A, Drummond AJ, Xie D, Baele G, Suchard MA. Posterior summarization in bayesian phylogenetics using tracer 1.7. Syst Biol. 2018;67(5):901–4.
56. Zhang Y. Mitochondrial genome rearrangement of Sesarmidae species and its phylogenetic implication. Zhoushan, China: Zhejiang Ocean University; 2022.
57. Moritz C, Dowling TE, Brown WM. Evolution of animal mitochondrial DNA: relevance for population biology and systematics. Annu Rev Ecol Syst. 1987;18(1):269–92.
58. Poulton J, Deadman ME, Bindoff L, Morten K, Land J, Brown G. Families of mtDNA re-arrangements can be detected in patients with mtDNA deletions: duplications may be a transient intermediate form. Hum Mol Genet. 1993;2(1):23–30.
59. Cantatore P, Gadaleta MN, Roberti M, Saccone C, Wilson AC. Duplication and remoulding of tRNA genes during the evolutionary rearrangement of mitochondrial genomes. Nature. 1987;329(6142):853–5.
60. Lavrov DV, Boore JL, Brown WM. Complete mtDNA sequences of two millipedes suggest a new model for mitochondrial gene rearrangements: duplication and nonrandom loss. Mol Biol Evol. 2002;19(2):163–9.
61. Sun S, Sha Z, Wang Y. Mitochondrial phylogenomics reveal the origin and adaptive evolution of the deep-sea caridean shrimps (Decapoda: Caridea). J Oceanol Limnol. 2021;39(5):1948–60.
62. Shen X, Li X, Sha Z, Yan B, Xu Q. Complete mitochondrial genome of the Japanese snapping shrimp Alpheus japonicus (Crustacea: Decapoda: Caridea): Gene rearrangement and phylogeny within Caridea. Sci China Life Sci. 2012;55(7):591–8.
63. Zhu L, Zhu Z, Lin Q, Zhu L, Wang D, Wang J. Characteristics and phylogenetic analysis of the mitochondrial genome in Palaemonidae. J Fish Sci China. 2017;28(7):852–62.
64. Zhang Z, Xing Y, Cheng J, Pan D, Lv L, Cumberlidge N, et al. In Phylogenetic implications of mitogenome rearrangements in East Asian potamiscine freshwater crabs (Brachyura: Potamidae). Mol Phylogenet Evol. 2020;143:106669.
65. Tan MH, Gan HM, Lee YP, Linton S, Grandjean F, Bartholomei-Santos ML, et al. ORDER within the chaos: Insights into phylogenetic relationships within the Anomura (Crustacea: Decapoda) from mitochondrial sequences and gene order rearrangements. Mol Phylogenet Evol. 2018;127:320–31.
66. Boore JL, Lavrov DV, Brown WM. Gene translocation links insects and crustaceans. Nature. 1998;392(6677):667–8.
67. Da Silva JM, Dos Santos A, Cunha MR, Costa FO, Creer S, Carvalho GR. Investigating the molecular systematic relationships amongst selected Plesionika (Decapoda: Pandalidae) from the Northeast Atlantic and Mediterranean Sea. Mar Ecol. 2013;34(2):157–70.
68. Chakraborty RD, Kuberan G. Notes on Plesionika alcocki (Anderson, 1896) and Plesionika narval (Fabricius, 1787) from the southern coast of India. Int J Fish Aquatic Stud. 2021;9(1):281–7.
69. Van Valen LM. A resetting of Phanerozoic community evolution. Nature. 1984;307(5946):50–2.
70. Benton MJ, Wu F. Triassic revolution. Front Earth Sci. 2022;10:899541.
71. Simms MJ, Ruffell AH. Synchroneity of climatic change and extinctions in the Late Triassic. Geology. 1989;17(3):265–8.
72 Dal Corso J, Bernardi M, Sun Y, Song H, Seyfullah LJ, Preto N, et al. Extinction and dawn of the modern world in the Carnian (Late Triassic). Sci Adv. 2020;6(38):eaba0099.
73. Dal Corso J, Mietto P, Newton RJ, Pancost RD, Preto N, Roghi G, et al. Discovery of a major negative δ13C spike in the Carnian (Late Triassic) linked to the eruption of Wrangellia flood basalts. Geology. 2012;40(1):79–82.
74. Ma L, Li J, Wang H, Yang J. Global jurassic source rocks distribution and deposition environment: lithofacies paleogeographic mapping research. Acta Geol Sin. 2014;88(10):1981–91.
75. Li S, Zhao Z, Hou Z. Tethyan changes shaped global animal distribution. J Hebei Univ(Natural Science Edition). 2021;41(5):551–64.
76. Von Rintelen K, Page TJ, Cai Y, Roe K, Stelbrink B, Kuhajda BR, et al. Drawn to the dark side: a molecular phylogeny of freshwater shrimps (Crustacea: Decapoda: Caridea: Atyidae) reveals frequent cave invasions

and challenges current taxonomic hypotheses. Mol Phylogenet Evol. 2012;63(1):82–96.
77. Larson RL. Latest pulse of Earth: evidence for a mid-Cretaceous superplume. Geology. 1991;19(6):547–50.
78. Schlanger SO, Jenkyns H. Cretaceous oceanic anoxic events: causes and consequences. Geol Mijnb. 1976;55:179–84.
79. Bralower TJ, Arthur MA, Leckie RM, Sliter WV, Allard DJ, Schlanger SO. Timing and Paleoceanography of Oceanic Dysoxia/Anoxia in the Late Barremian to Early Aptian (Early Cretaceous). Palaios. 1994;9(4):335–69.
80 Leckie RM, Bralower TJ, Cashman R. Oceanic anoxic events and plankton evolution: biotic response to tectonic forcing during the mid-Cretaceous. Paleoceanography. 2002;17(3):13-1-13–29.

Publisher's Note